Progress in Oceanography 218 (2023) 103128

Contents lists available at ScienceDirect

Progress in Oceanography

journal homepage: www.elsevier.com/locate/pocean

Seasonal dynamics of sea-ice protist and meiofauna in the northwestern Barents Sea

Miriam Marquardt [a,*], Lucie Goraguer [a,b], Philipp Assmy [b], Bodil A. Bluhm [a], Signe Aaboe [c], Emily Down [c], Evan Patrohay [a], Bente Edvardsen [d], Agnieszka Tatarek [e], Zofia Smoła [e], Jozef Wiktor [e], Rolf Gradinger [a]

[a] Department of Arctic and Marine Biology, UiT The Arctic University of Norway, Tromsø, Norway
[b] Norwegian Polar Institute, Fram Centre, Tromsø, Norway
[c] Norwegian Meteorological Institute, Fram Centre, Tromsø, Norway
[d] Section for Aquatic Biology and Toxicology, Department of Biosciences, University of Oslo, Oslo, Norway
[e] Institute of Oceanology, Polish Academy of Sciences, Sopot, Poland

ARTICLE INFO

Keywords:
Sympagic
Sea-ice biota
Seasonality
Foraminifers
First-year ice
Ice drift
Barents Sea

ABSTRACT

The rapid decline of Arctic sea ice makes understanding sympagic (ice-associated) biology a particularly urgent task. Here we studied the poorly known seasonality of sea-ice protist and meiofauna community composition, abundance and biomass in the bottom 30 cm of sea ice in relation to ice properties and ice drift trajectories in the northwestern Barents Sea. We expected low abundances during the polar night and highest values during spring prior to ice melt. Sea ice conditions and Chlorophyll *a* concentrations varied strongly seasonally, while particulate organic carbon concentrations were fairly stable throughout the seasons. In December to May we sampled growing first-year ice, while in July and August melting older sea ice dominated. Low sea-ice biota abundances in March could be related to the late onset of ice formation and short time period for ice algae and uni- and multicellular grazers to establish themselves. Pennate diatoms, such as *Navicula* spp. and *Nitzschia* spp., dominated the bottom ice algal communities and were present during all seasons. Except for May, ciliates, dinoflagellates, particularly of the order *Gymnodiales*, and small-sized flagellates were co-dominant. Ice meiofauna (here including large ciliates and foraminifers) was comprised mainly of harpacticoid copepods, copepod nauplii, rotifers, large ciliates and occasionally acoels and foraminifers, with dominance of omnivore species throughout the seasons. Large ciliates comprised the most abundant meiofauna taxon at all ice stations and seasons (50–90 %) but did not necessarily dominate the biomass. While ice melt might have released and reduced ice algal biomass in July, meiofauna abundance remained high, indicating different annual cycles of protist versus meiofauna taxa. In May highest Chlorophyll *a* concentrations (29.4 mg m^{-2}) and protist biomass (107 mg C m^{-2}) occurred, while highest meiofauna abundance was found in August (23.9 × 10^3 Ind. m^{-2}) and biomass in December (0.6 mg C m^{-2}). The abundant December ice biota community further strengthens the emerging notion of an active biota during the dark Arctic winter. The data demonstrated a strong and partially unexpected seasonality in the Barents Sea ice biota, indicating that changes in ice formation, drift and decay will significantly impact the functioning of the ice-associated ecosystem.

1. Introduction

Arctic marine biota and upper ocean ecosystems are, by nature, finely tuned to strong seasonality, particularly concerning light, and show large fluctuations in terms of production and composition over the year (Sakshaug et al., 2009; Leu et al., 2015). The timing of ice formation and melt and the thickness and origin of ice floes affect not only the seasonality of biological processes, e.g. productivity, timing of ice algae and phytoplankton blooms and the match/mismatch with ice fauna and zooplankton grazers (Melle and Skjoldal, 1989; Hansen et al., 2003; Søreide et al., 2010; Leu et al., 2011), but also the biodiversity (Bluhm et al., 2018; Hop et al., 2020; Ehrlich et al., 2020). Sea-ice biota

* Corresponding author.
E-mail address: miriam.marquardt@uit.no (M. Marquardt).

https://doi.org/10.1016/j.pocean.2023.103128

Available online 27 September 2023

represents an important link in the carbon transfer to pelagic and benthic ecosystems (referred to as sympagic-pelagic-benthic coupling). Highly seasonal ice algal primary production, ice fauna grazing on algae, and release of algal aggregates (Riebesell et al., 1991; Assmy et al., 2013; Boetius et al., 2013) and fecal pellets strongly contribute to the carbon flux in the Arctic Ocean (Gradinger et al., 1999; Nozais et al., 2001; Søreide et al., 2010; Fadeev et al., 2021). However, many ecosystem connections and processes over the annual cycle are not well understood. For example, unexpectedly high biological activity has been observed during the previously assumed dormant polar night (Vader et al., 2015; Berge et al., 2015; Grenvald et al., 2016). Further, knowledge gaps exist regarding sympagic communities outside the well-studied spring and especially summer months (Hegseth and von Quillfeldt, 2022 and references therein; Bluhm et al., 2018 and references therein) including the recruitment and seeding processes of sea-ice biota in the late winter/early spring (Olsen et al., 2017; Kauko et al., 2018; Gradinger and Bluhm, 2020). The ongoing environmental changes of sea ice growth, melt and large-scale ice disappearance (Comiso et al., 2008; Stroeve and Notz, 2018; Kwok, 2018) as well as the disruption of long-range sea ice transport (Krumpen et al., 2019) necessitate a deeper understanding of ice-associated ecosystem. These changes can lead to indirect or direct cascading effects on the Arctic food web (Kovacs et al., 2011; Barber et al., 2015; Krumpen et al., 2019; Stige et al., 2019; Pagano and Williams, 2021), altering the biological and biogeochemical processes related to the sea ice system in terms of biodiversity, production and seasonality of the biota inhabiting the sea ice.

This study focuses on the structure of sea-ice biota in the Barents Sea across seasons and its relationship to ice origin under varying environmental conditions. Although the Barents Sea is one of the better monitored Arctic seas (Siwertsson et al., 2023), the seasonal evolution of the Barents Sea marine ecosystem is still poorly known, mainly due to restricted accessibility of the seasonally ice-covered area in winter and early spring. The Barents Sea is a relatively shallow shelf sea situated in the transition zone between the sub-Arctic and the Arctic. It is, throughout the year, influenced by warmer Atlantic water masses in the south, while the surface layers in the north represent fresher and colder Arctic water entering from the Nansen Basin (Loeng, 1991; Smedsrud et al., 2010). The Barents Sea ice cover is dominated by annual pack ice, mainly locally formed but also imported with large variability through the eastern passage between Franz Jozef Land and Novaya Zemlya (Lind et al., 2018; Efstahiou et al., 2022). Multiyear ice from the Central Arctic Ocean contributes only sporadically (Kwok, 2009; Lind et al., 2018). Sea ice typically forms in winter (November) and begins to melt in late spring (April-May) with an annual maximum sea-ice extent of 532×10^3 km^2 (April 2021) and annual minimum extent of 16×10^3 km^2 in September (2021) (OSI SAF, 2023). Similar to other Arctic seas, the Barents Sea has experienced sea ice reduction over the last decades (Årthun et al., 2012; Onarheim and Årthun, 2017; Barton et al., 2018), especially in winter (Isaksen et al., 2022). While increased advection of Atlantic water masses ("Atlantification", Asbjørnsen et al., 2020; Ingvaldsen et al., 2021) can explain the sea ice reduction in the eastern Barents Sea (Årthun et al., 2012) and north of Svalbard (Duarte et al., 2020), a change of northerly winds and ice import has affected its northwestern parts (Screen and Simmonds, 2010; Lind and Ingvaldsen, 2012; Lind et al., 2018; Dörr et al., 2021; Efstahiou et al., 2022). Overall, the northern Barents Sea is changing from a cold and stratified Arctic regime to a warmer and more mixed Atlantic-influenced regime with drastically changing ice conditions (Lind et al., 2018; Aaboe et al., 2021). The weakened stratification and delayed formation of the ice cover in autumn allow for a larger heat flux from the warmer ocean to the atmosphere (Lind et al., 2018; Isaksen et al., 2022). In summer, the ocean receives more sunlight due to the decreased ice coverage. These warming trends are accompanied by an increase in precipitation and extreme weather events in the Arctic potentially linked to extreme weather at lower latitudes (Cohen et al., 2020; Moon et al., 2023).

Sea ice is recognized as an important feeding habitat and hunting ground for a variety of small and large animals as well as humans, with somewhat varying roles across seasons (Carey, 1985; Melnikov, 1997; Ainley et al., 2003; Wassmann et al., 2011; Hop et al., 2019, 2021; Møller and Nielsen, 2020; Hegseth and von Quillfeldt 2022). The physical properties of sea ice allow the growth of a network of brine channels, a habitat with extreme seasonal as well as vertical changes in temperature, salinity, light and nutrient concentration (Arrigo, 2016; Petrich and Eicken, 2016). At any time of ice cover, the brine channels can host a wide variety of uni- and multicellular organisms (Carey, 1985; Gradinger, 1999; Marquardt et al., 2011, Bluhm et al., 2018) that can be allochthonous (temporary) or autochthonous (permanent) to the sea-ice habitat (Carey, 1985; Gulliksen and Lønne, 1989). The highest densities of biota are often found in the bottom 20–30 cm of the ice where free exchange with nutrients from the underlying seawater can sustain substantial growth of algal biomass (Gradinger, 2009). The environmental conditions are generally most stable at the water–ice interface in all seasons, while conditions become more extreme (e.g., in nutrient availability, temperature, brine salinity, permeability, snow cover; Arrigo, 2016) in the ice interior and towards the ice-snow interface as air temperatures drop in winter. This, in turn, limits the vertical distribution of biota within the ice (Arrigo and Sullivan, 1992; Mundy et al., 2005, 2007). Similar to arctic phytoplankton spring bloom patterns, the ice protists often show a seasonal pattern, with diatoms often dominating the ice assemblages (Syvertsen, 1991; Ratkova and Wassmann, 2005; Lund-Hansen et al., 2017; Assmy et al., 2023) in the spring. Later in summer flagellated taxa can also contribute a significant fraction (e.g., Gradinger, 1999) when nutrients are limiting for diatom growth in the ice, or diatoms attached to the bottom sea ice have been washed out (Assmy et al., 2013). In the Barents Sea pennate diatoms such as *Nitzschia frigida* are predominant (e.g., Niemi et al., 2011; Hegseth and von Quillfeldt, 2022), but the community composition can also vary depending on ice properties such as ice age. *Nitzschia frigida* has been suggested as an indicator species for first-year ice and *Melosira arctica* for multiyear ice (Syvertsen, 1991; Hop et al., 2020). Sea ice algae contribute to primary production with <5 up to 30 and even 50 % in different regions of the Arctic (Central Arctic Ocean - Gosselin et al., 1997; and Fernández-Méndez et al., 2015; North of Svalbard – Ehrlich et al., 2021; Chukchi Sea – Feng et al., 2021), with estimates of up to 20 % in the northern Barents Sea (Hegseth, 1998). In high latitudes, light is one of the main factors limiting the growth of primary producers (Sherr et al., 2003; Sakshaug et al., 2009; Hodal et al., 2012). With the return of light in early spring, shade-adapted ice algae species start growing under very low light conditions (Johnsen and Hegseth, 1991; Mock and Gradinger, 1999; Mundy et al., 2005; Hancke et al., 2018) and the ice algal biomass usually accumulates by May (around 80°N, Leu et al., 2011). The phytoplankton spring bloom is then initiated by melting ice in June/July in seasonal ice zones (Smetacek and Nicol, 2005; Sakshaug et al., 2009; Leu et al., 2011; Hodal et al., 2012). However, phytoplankton blooms below consolidated sea ice seem to become more frequent as the ice cover is getting thinner and melts earlier (Arrigo et al., 2012; Assmy et al., 2017; Ardyna et al., 2020).

A taxonomically diverse range of heterotrophic organisms from bacteria, flagellates, ciliates and sea-ice (or sympagic) meiofauna can feed on ice bacteria, algae and various heterotrophs (Carey, 1985; Grainger and Hsiao, 1990; Gradinger et al., 1999; Bluhm et al., 2018). Commonly observed sea-ice associated metazoans are copepods (mainly harpacticoids and cyclopoids) as well as copepod nauplii stages, rotifers, nematodes, acoel flatworms and occasionally meroplankton for instance polychaete larvae (Marquardt et al. 2011; Bluhm et al., 2018 and references therein). The community structure of ice meiofauna is often related to water depth (shelf versus basin), ice properties (e.g., temperature and salinity tolerance levels) and as well as ice age (first-year ice versus multiyear ice) (Bluhm et al., 2018; Patrohay et al., 2022 and references therein). Due to more stable conditions and easiest access of colonization from the pelagic and benthic habitats, highest abundances of meiofauna usually co-occur with high ice algae densities (i.e., food

availability) in the lowermost bottom centimeters of the ice (Friedrich, 1997; Nozais et al., 2001; Arndt and Swadling, 2006; Marquardt et al., 2011). A diverse range of metazoan eggs in the sea-ice channels (Werner and Hirche, 2001; Marquardt et al., 2011; Ehrlich et al., 2021) also points towards the importance of the sea ice also as a nursery ground. The taxonomic composition of the ice biota and indicators of reproduction in sea ice can provide a second line of indirect evidence of ice origin and longevity, in addition to back-tracking of floes. For example, the presence of benthic-origin fauna points towards origin in shallow areas rather than the deep central Arctic basin (Arndt et al., 2009; Marquardt et al., 2011).

Our study goals were to characterize sea-ice biota including eukaryotic microalgae, and uni- and multicellular heterotrophs over the entire seasonal cycle, along a latitudinal gradient in the northwestern Barents Sea. We expected different patterns in seasonality of protist and meiofauna abundance and biomass based on different life history strategies. Specifically, we anticipated autotrophic algae (and corresponding chlorophyll *a* biomass) to peak in spring (May) and summer (August) and algae-grazing meiofauna, here including large ciliates and foraminifers, to respond with some delay. Further, we expected that differences in physical ice properties, and origin and age of the sea-ice floes would in part explain community structure differences in both protist and meiofauna communities. Specifically, we hypothesized that protist taxa characteristic of mature sea-ice communities would prevail in older ice (indicated by lower bulk salinities and long duration of drift). Furthermore, we hypothesized that meiofauna would be dominated by pelagic taxa where ice originated over deep water, while it would contain a higher fraction of benthic taxa where ice originated over shallower shelves.

2. Material & methods

2.1. Study area and ice sampling

This study was part of the Nansen Legacy project (arvenetternansen.no, Wassmann, 2022). Sampling onboard R/V Kronprins Haakon was repeated along a latitudinal transect in the northwestern Barents Sea during four contrasting seasons: August (Cruise ID: Q3) and December 2019 (Cruise ID: Q4), March 2021 and 2022 (Cruise IDs: Q1/JC3), May (Cruise ID: Q2) and July 2021 (Cruise ID: JC2-1) (Fig. 1, Table 1). The gap in 2020 was not intended, but a consequence of the COVID-19 pandemic. The cruise reports, providing overviews and details regarding the entire science mission of each cruise, are available at: https://septentrio.uit.no/index.php/nansenlegacy/section/view/cruise-reports.

At ice-covered stations, ice cores were taken for the determination of abundance and biomass of sea-ice meiofauna and protists (lowermost 30 cm) as well as for environmental variables (full cores: ice temperature, bulk salinity, Chlorophyll *a* (Chla) and particulate organic carbon (POC) and nitrogen (PON) concentrations. Ice cores were taken from undeformed level ice areas with a KOVACS ice corer (Mark II coring system, inner diameter 9 cm). For each core, snow and ice thickness and freeboard were determined (Table 1). Within tents for light protection, cores for Chla, POC and PON were sliced on a cutting board into the following sections, given as distance from the ice-water interface: 0–3 cm (bottom ice layer), 3–10 cm, 10–20 cm, 20–30 cm, and in 20 cm intervals from there onwards to the top. For the lowermost 50 cm of the cores the matching segments of five ice cores were pooled for Chla, POC and PON. Above 50 cm core length only sections from two of the five cores were used for pooling due to the larger volume of the 20 cm sections. Three additional ice cores were taken at each station for sea-ice protist and meiofauna analysis, using the same sectioning but focusing on the lowermost 30 cm only. All ice sections were put into containers and then brought onboard for further processing. For bulk salinity and ice temperature section and measurement intervals see Section 2.3.

2.2. Onboard sea-ice sample processing (Chla, POC/PON, ice protists and meiofauna)

All sea-ice core sections were melted in the dark and at 4 °C within 24–28 h, and 100 ml filtered seawater (<0.22 μm) was initially added per 1 cm section to reduce negative impacts related to osmotic stress. In

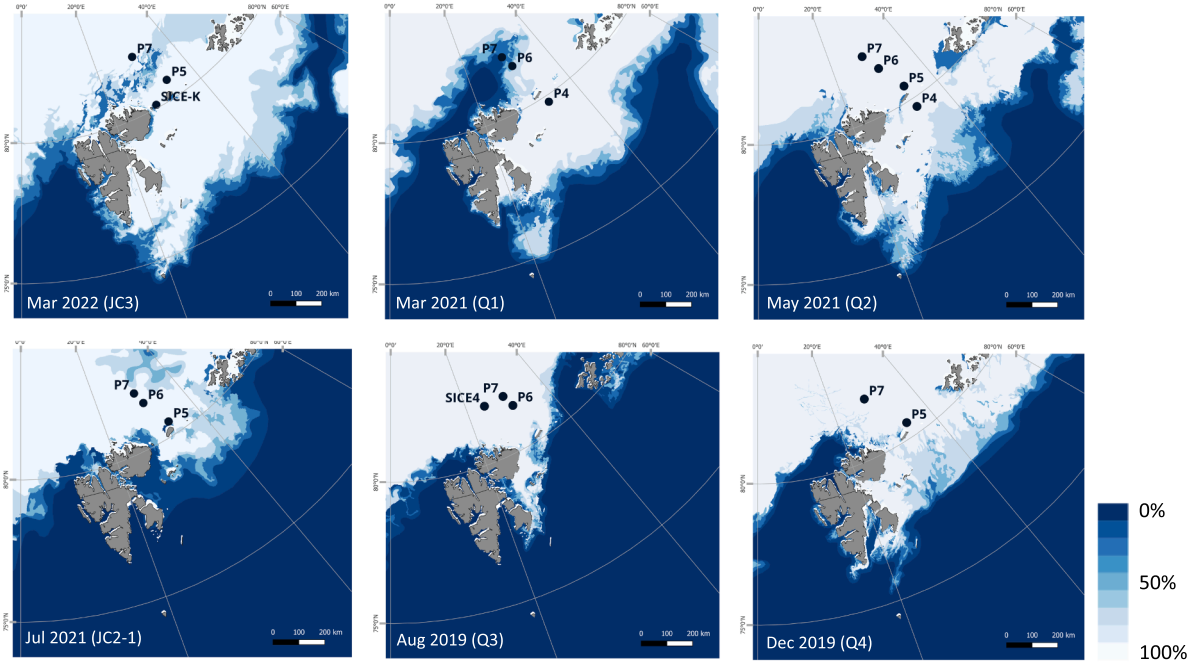

Fig. 1. Study area and station overview in the northwestern Barents Sea from August 2019 to March 2022. Lower left in each panel the month, year and cruise ID are given. Daily sea ice concentrations (%) from every 1st of the month in white and open water in blue. Data obtained from MET Norway/E.U. Copernicus Marine Service Information; https://doi.org/10.48670/moi-00128 and plotted with the mapping software QGIS 3.28.2.

Table 1
Station overview for sea ice sampling in the Barents Sea. Mean ice core length (ICL), ice thickness (IT) and freeboard (F) were from n = 3 replicates, snow thickness (ST) from n = 9 measurements. Ice age (FYI = first-year ice, SYI = second-year ice) was assigned according to bulk salinity profiles (figures in S1) and NSIDC ice age distribution data (Tschudi et al., 2019). Mean ice concentration (conc., %) is averaged over the four-week period preceding the sampling date (data from Steer and Divine, 2023). ND: not determined.

Cruise	Station	Date	Latitude	Longitude	ICL (cm)	IT (cm)	F (cm)	ST (cm)	Ice age	% ice conc.
Q1	P4	11-3-21	79.7720	33.6729	52.5		1	15.5	FYI	97 ± 3
Q1	P6	15-3-21	81.5396	31.1004	50	48.8	3	9	FYI	28 ± 34
Q1	P7	17-3-21	81.9994	29.9936	47	44	2.5	3.5	FYI	20 ± 35
JC3	P5	27-2-22	80.6865	33.9812	35	34	3	1.5	FYI	ND
JC3	P7	2-3-22	82.0386	29.8910	39	38	−1	13	FYI	ND
JC3	SICE-K	7-3-22	80.1205	29.2725	53.5	53	1	18	FYI	ND
Q2	P4	5-5-21	79.6782	33.5265	22.5	21.5	0	6	FYI	71 ± 33
Q2	P5	8-5-21	80.5439	33.6217	60	59	−1	13.5	FYI	96 ± 4
Q2	P6	10-5-21	81.5626	30.8294	96.5	96	4	12	FYI	92 ± 7
Q2	P7	13-5-21	82.2273	28.6964	120.5	120	10	4.5	FYI	96 ± 4
JC2-1	P5	20-7-21	80.5002	33.4216	114	120	12	2	FYI/SYI	95 ± 6
JC2-1	P6	22-7-21	81.5255	30.8165	109	107	8	2	FYI/SYI	94 ± 7
JC2-1	P7	25-7-21	81.9845	30.0223	118	120	9	4.5	FYI/SYI	85 ± 23
Q3	P6	17-8-19	81.5327	30.9684	104	108	9	12	FYI/SYI	96 ± 4
Q3	P7	20-8-19	81.9861	29.9957	129	128	9	5	FYI/SYI	96 ± 5
Q3	SICE4	23-8-19	81.9783	24.6400	166	159	17	9	ND	ND
Q4	P5	6-12-19	80.5333	34.3877	39	35	0	8	FYI	88 ± 14
Q4	P7	2-12-19	82.0428	28.7516	118	112	8	13	FYI	98 ± 2

a few instances, when time was lacking, samples were melted at room temperature, while being continuously monitored and mixed to ensure homogenous salinity and low temperature. Total sample volume was recorded.

After complete melt, Chla samples were filtered onto GF/F glass microfiber filters (Whatman, England) and immediately extracted in 5 ml of methanol in darkness at 4 °C for ca. 24 h (Holm-Hansen and Riemann, 1978) and measured onboard with a Triology fluorometer (Turner, USA; final data: Vader et al. 2022a–e and March 2022 data in Vader et al., unpublished).

Melted samples for POC/PON were filtered onboard onto pre-combusted Whatman GF/F filters. The limited volume of melted sea ice allowed typically only one but occasionally triplicate pseudo-replicates (500–1500 ml per replicate). Filters were stored at −20 °C and analyzed within 1 year on a CE 440 Exeter analytical CHN Analyzer (Reigstad et al., 2008). Mean values and standard deviations were calculated for POC and PON values and the C:N ratio was calculated. PON values <3× the blank values were excluded from the dataset. POC/PON datasets were made available by Marquardt et al. (2022a–f).

The melted ice protist/meiofauna core sections were carefully mixed before taking a 90 ml subsample for protist identification and quantification. These samples were fixed with 25 % electron microscopy grade glutaraldehyde (0.1 % final concentration) and 20 % hexamethylenetetramine-buffered formalin solution (1 % final concentration) and stored in brown glass bottles. These samples were stored at room temperature until shipment to the Institute of Oceanology, Polish Academy of Sciences Poland (IOPAN) for microscopic analyses. The entire remaining volume was concentrated over a 20 μm sieve for meiofauna. When time allowed, sea-ice meiofauna were identified and counted alive onboard with Leica stereomicroscope (M80, 7.5–60× or M125, 7.8–160× magnification). Otherwise, samples were fixed (2 cores by adding 37 % formaldehyde for a final concentration of 2 %, 1 additional core by addition of 96 % Ethanol for a 95 % final concentration) and stored for further analysis in the lab at UiT The Arctic University of Norway (Tromsø).

2.3. Ice biota measurements: Determination of abundance, composition, and biomass of sea-ice protists and meiofauna

Depending on the density of the sample, a volume of 10–50 ml (when high sediment load: 3 ml) was settled in Utermöhl sedimentation chambers (Hydro-Bios, Kiel, Germany) for 48 h to study sea-ice protists. Cells were counted and identified to lowest possible taxonomic level using an inverted Nikon Ti-S and TE300 light microscope at 100–600× magnification depending on the size of the species (Edler and Elbraechter, 2010). All organisms were counted in scaled fields of view along transects, across the entire chamber area. When the number of cells was below 400–500 using this approach, the entire chamber was counted. Except for protist data from March 2022 (Assmy et al., unpublished), the sea-ice protist data are published in Assmy et al. (2022a–d) and Wold et al. (2022).

Counting, identification and documentation of sea-ice meiofauna in the fixated samples were performed with a Leica M205C stereomicroscope (8×–160× magnification) at UiT. Specimens were identified to the lowest taxonomic level possible. Large ciliates and other large protists (>20 μm, e.g., foraminifers) were also counted in alive and fixated samples and are included as “meiofauna” in this study. However, in the fixated samples they may be underestimated when high amounts of algae aggregates and debris obscured them in the samples. Eggs were counted in order to study reproduction patterns. Since no classification keys are available for the identification of eggs, they were sorted into morphotypes. Sea-ice meiofauna counts, abundance and biomass are published in Marquardt et al. (2023a–e).

Sea-ice protist and meiofauna abundance per liter of melted sea ice were calculated by dividing the number of cell counts in each sample by the total volume of the ice core sections (added filtered seawater was removed). For the abundance in cells m^{-2}, the abundance per liter of melted of sections of sea ice was divided by the ice core area “A” ($A = \pi \times r^2 = 0.006317\ m^2$) where r is the radius of the core The integrated number of cells for the lowermost 30 cm of the ice core was calculated by summing the cell counts of the individual ice core sections analyzed (given as abundance in Ind. m^{-2}). The vertically integrated biomass (0–30 cm) for sea-ice protists and meiofauna (mg C m^{-2}) was determined per taxon by multiplying abundances by the carbon content per cell or individual. Sea-ice protists carbon content was derived from biovolumes estimated using geometric equations (Hillebrand et al., 2002) and converted to carbon content per cell (Menden-Deuer and Lessard, 2000). Individual carbon contents for ice meiofauna taxa were based on literature summarized in Ehrlich et al. (2021), and carbon values for foraminifers were provided by de Freitas et al. (2021) for benthic species (*Bolivinia* sp.: 0.00875 μg C $Ind.^{-1}$; *Elphidium* sp.: 0.126 μg C $Ind.^{-1}$) and Anglada-Ortiz et al. (2023) for the pelagic species *Neogloboquadrina pachyderma* (0.0013 μg C $Ind.^{-1}$).

2.4. Ice physical measurements (bulk salinity, ice in situ temperature, brine salinity and volume) and ice trajectories

The top 20 cm of the salinity core was cut into 5 cm thick segments (0–5 cm, 5–10 cm, etc.), while from 20 cm to the bottom of the core, it was cut into 10 cm intervals. Sections were melted in containers in the dark at room temperature. After complete melt, the bulk salinity of the ice-core sections was measured with a WTW 3310 conductivity sensor. Ice in situ temperature was measured immediately after coring using a VWR temperature sensor to take measurements in the drilled holes over the entire ice thickness, (The Nansen Legacy 2022, Version 10–14.17.1), starting at 2.5 cm from the top of the ice in 10 cm intervals. Salinity and temperature data are available in Jones et al. (2023).

The brine salinity and brine volume fraction were calculated for each ice section using the equations given by Cox and Weeks (1983) and Leppäranta and Manninen (1988) based on the sea-ice bulk salinities and sea-ice temperature data. Ice age was determined (FYI = first-year ice, SYI = second-year ice, Table 1) according to bulk salinity profiles (Fig. S1) and NSIDC ice age distribution data (https://nsidc.org/data/nsidc-0611/versions/4).

Trajectories of the locations of the on-ice stations were calculated backwards in time from daily gridded sea-ice drift and concentration data. The ice location was tracked in a Lagrangian manner by calculating the location of the ice station in daily steps backward in time according to the sea-ice drift resampled to the current location of the ice station. This was conducted similarly to the method described by Kimura et al. (2020) but tracking backwards in time instead of their forward tracking. At each daily timestep, the sea-ice concentration was retrieved at the ice station location, and the trajectory was ended when the condition of ice concentration below 50 % was met for three consecutive timesteps. An extension to the trajectory is shown as a dotted line to where the condition of ice concentration below 15 % is met for three consecutive timesteps, in order to give some idea about the likely range of endpoints of the trajectories.

All sea-ice data used in the backtracking are from the EUMETSAT Ocean and Sea Ice Satellite Application Facility (OSI SAF, https://osi-saf.eumetsat.int/). The sea-ice drift data was derived from multiple passive microwave sensors. The sea-ice drift climate data record version 1 (OSI SAF, 2022a) was used for dates up to and including 2020, and the sea-ice drift near real time product (OSI SAF, 2010) for dates from 2021 onwards. The sea-ice concentration was also based on selected passive microwave sensors. The sea ice concentration climate data record version 3 (OSI SAF, 2022b) was used for dates up to and including 2020, and the accompanying interim climate data record version 3 (OSI SAF, 2022c) for dates from 2021 onwards.

In Fig. 2, the sea-ice trajectories are shown together with a background of ice age at the closest time to the sampling at the locations. The sea-ice age data is from Tschudi et al. (2019) and covers the period up to December 2021. For stations after 2021, the sea-ice type from Copernicus Climate Change Service (C3S) was used instead (C3S, 2023).

The sea-ice drift products have spatial resolutions of 75 km (climate data record) and 62.5 km (near real time product) and therefore neither the products nor the calculated trajectories can necessarily capture the correct behavior and history of an individual ice floe. In addition, there is uncertainty in the ice drift product, which will accumulate the further back in time the trajectory reaches. Finally, there is significant uncertainty about the exact endpoint of the trajectory, which here was ended at 50 %–15 % ice concentration where only a corresponding percentage of the ice parcels will still be over ice. The trajectories therefore contribute to an overall picture of how the ice has moved on a large scale but cannot be taken as precise for an individual ice floe. Finally, the trajectories were cut when backtracked into a masked region which reaches approximately 100 km from land, based on a landmask from the drift product. This especially affects ice stations close to Kvitøya or Edgeøya (see Fig. 2) where some stations have very short trajectories or could not be tracked at all due to trajectory trimming in coastal regions.

2.5. Statistical and traits analyses

Plots and statistical analysis were performed with RStudio (version 2023.03.0 + 386) using R-basis (version 4.2.3) and following packages: vegan (2.6.4, Oksanen et al., 2022), ggplot2 (3.4.1, Wickham, 2016) tidyverse (2.0.0, Wickham et al. 2019), devtools (2.4.5, Wickham et al., 2022), corr (0.4.4, Kuhn et al., 2022), corrplot (0.92, Wei and Simko, 2021), reshape2 (1.4.4, Wickham, 2007) and psych (2.3.3, Revelle, 2023).

A Spearman correlation test (S2.1) was run to test for significant correlations between variables followed by a Correspondence Analysis (CA) and a Canonical Correspondence Analysis (CCA) to visualize community similarity patterns across seasons. The CA and CCA was performed separately for both integrated abundance and biomass values (for the integrated lowermost 30 cm) of sea-ice protist (family level) and, separately, meiofauna (large group level, mainly Phylum except for "Copepod nauplii" and "Harpacticoids") datasets. Meiofauna and protist datasets were square-root transformed before analysis and environmental data were standardized (scale "x", the community data matrix, to zero mean and unit variance) with the "decostand" command in R. Significant (significance level of alpha = 0.05) environmental parameters were fitted onto the ordinations (S2.2).

One-way PERMANOVAs were run to test for significant differences in community structure (based on abundance data) between different factors and variables (see S2.3) based on the Bray Curtis Similarity (permutations: 9999).

Once taxa were identified, a biological traits analysis was conducted for sea-ice meiofauna using a total of 6 traits (body length, body width, salinity tolerance, temperature tolerance, feeding mode, and diet) representing a total of 29 modalities. The trait-by-taxon matrix was compiled using Patrohay et al. (2022). Information on taxa found in the study area but missing in Patrohay et al. (2022) was gathered through a literature review and affinity to trait modalities was assigned using fuzzy coding with 0 representing no affinity to a given modality, 1 and 2 indicating partial affinity and 3 indicating full affinity (Chevenet et al., 1994). A trait-by-station matrix was then created for each seasonal sampling campaign by multiplying the proportional taxonomic abundances at each station by the traits-by-taxon matrix following the procedures outlined in Degen et al. (2018).

3. Results

3.1. Seasonality of environmental conditions at sea-ice stations and ice cover

The mean sea ice concentration at most sampled locations varied between 71 and 98 % (Table 1), with the exceptions of lower values (20–28 %) at the northernmost stations P6 (near the shelf break where Atlantic Water flows in) and P7 (in the Nansen Basin) in March 2021. The calculated ice trajectories indicated that the young pack ice sampled in March 2021 and 2022 was locally formed on the Barents Shelf in the northeast near Franz Jozef Land (elapsed drift time: <60 days; ice trajectories in Fig. 2. At the southern shelf stations P4 (in 2021, Fig. 2a) and P5 (in 2022, Fig. 2b), the ice was potentially young ice that was seasonally formed (elapsed time: <10 days, Fig. 2). Note, that these two stations were located close to Kvitøya and therefore their trajectories were trimmed due to the landmask. However, in a test, allowing the trajectories to cross-over coastal regions still gave elapsed time <100 days. Overall, these results agree with the bulk salinity profiles showing relatively high values throughout the core vertical profile, typical for FYI but with potential loss or melt of the lowermost bottom centimeters causing low values at the bottom (Fig. S1).

In May 2021 all sea ice was considered FYI, with slightly older ice floes (about 200 days ice drift, Fig. 2c and Fig. S1) at stations P6 and P7 starting the drifting from the northeastern Nansen Basin northeast of Franz Josef Land into the Barents Sea. The ice pack at the shelf stations

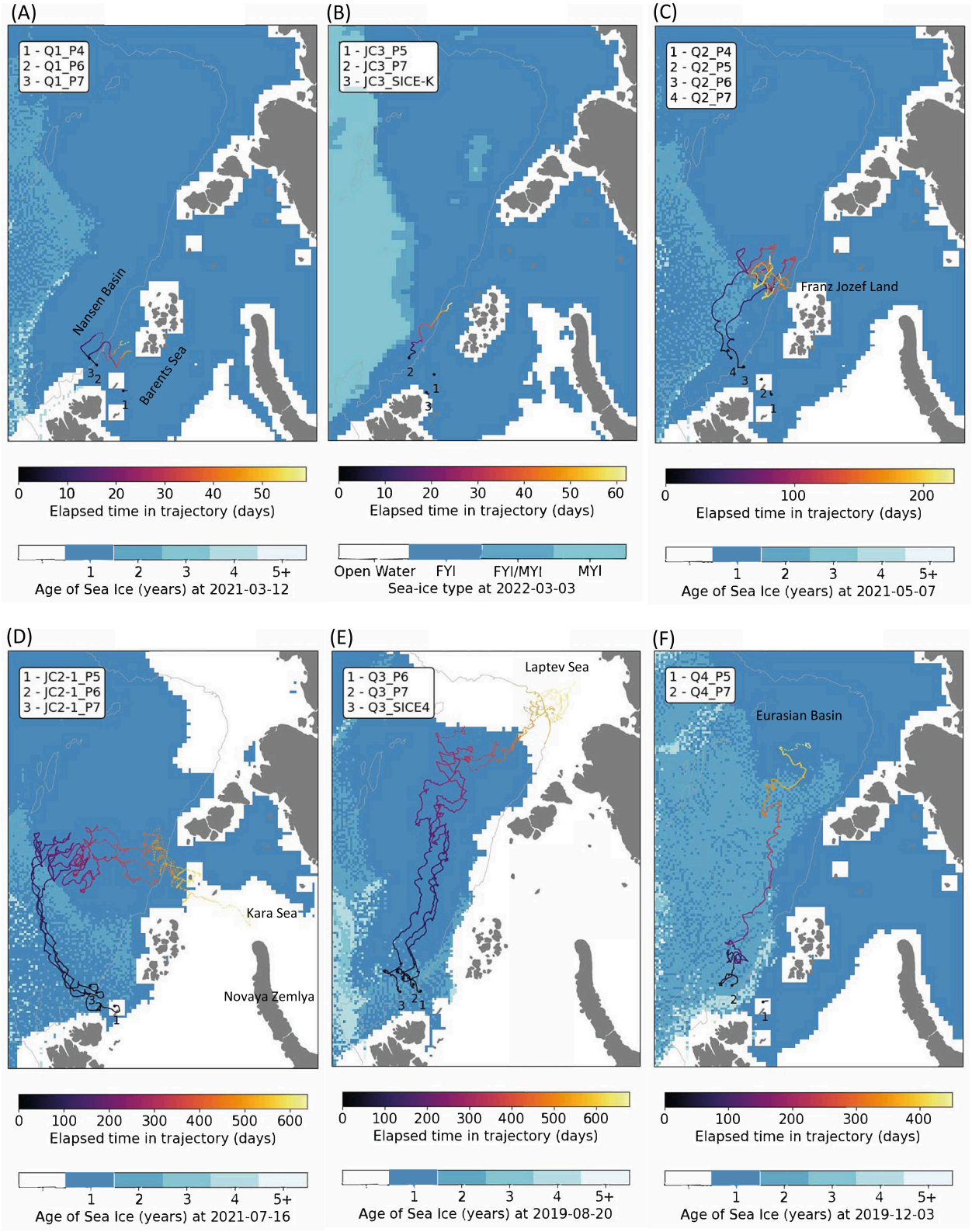

Fig. 2. Drift trajectories of the ice stations from the study sites in March 2021 (A), March 2022 (B), May 2021 (C), July 2021 (D), August 2019 (E) and December 2019 (F). The estimated trajectories (colored lines, first colorbar: elapsed time in trajectory) are tracked backwards in time by using OSI SAF sea-ice drift and concentration data (OSI SAF, 2010, 2022a,b,c, see Section 2.4) from the years 2019–2022. Numbers on the map at each trajectory indicate the stations (their names given in the inset legend) and the location of the start point for backtracking. The background field, and the second colorbar, present the age of sea ice given in years (or age classes in (B)) from the closest data to the mean sampling date of the sites (data from NSIDC 2019, C3S 2023, see Section 2.4). The white color in these maps shows both open water and coast masking in the age and type fields. Grey solid lines indicate the 1000 m bathymetry contour and the entrance to the Arctic basin area. Names of locations referred to in the text (Section 3.1) are included in the map.

P4 and P5, in contrast, was younger (<50 days) and originated locally, however also here the ice pack at the two shelf stations was too close to land to be fully tracked. The mean drift field suggests that the sea ice at these locations would be approximately the same age, or less, as two northern stations. In July 2021 (Fig. 2d), the SYI with lower bulk salinities originated from the Kara Sea shelf east of Franz Jozef Land within 500–600 days earlier and drifted over the northeastern Nansen Basin into the Barents Sea. Similar to July, the August pack ice had drifted for 400–600 days, originating in the Laptev Sea (P6 and P7, Fig. 2e) or nearby over the Eurasian Basin (SICE4). Older ice age estimates are also supported by the low bulk salinity values in the vertical profiles indicating old FYI or SYI. In December 2019 (Fig. 2f), the trajectories indicated a north south difference with older ice around the P7 station (400 days of drift) coming from the northeastern Nansen Basin, while ice at P5 had potentially formed locally (<50 days) but also here the near-land location is the reason for the short trajectory.

Ice thickness varied between stations and seasons. Generally, we found younger and thinner ice (<50 cm) in March and early May, while later in May and in the summer the sea ice encountered was over 100 cm thick (Table 1) agreeing with estimated older ice age based on drift and bulk salinities (see above). The sea-ice floes in December were very heterogeneous with mean ice thickness of 35 cm at station P5 and 112 cm at station P7. Freeboard varied between −1 and 8 cm in December, March and early May, while from mid-May to August it ranged from 8 to 17 cm (Table 1). Snow thickness varied between stations and with seasons, with lowest snow depth of 1.5 cm in March 2022 (JC3 – P5) and 2.0 cm in July (JC2-1 – P5 and P6). Highest average snow depth was measured in March 2021 (Q1 – P4) with 15.5 cm and in May (Q2 – P5) with 13.5 cm.

Vertical profiles of ice in situ temperatures, brine salinity and brine volume at the different stations are presented in Fig. S1. Sea ice was coldest in March (2021 and 2022 between < −5 °C and −11 °C) and December (e.g., at P5 –12 °C top cm) in the top centimeters of the ice and gradually increased towards the ice-water interface. The temperature was close to the freezing point of sea water (around – 2 °C) in the lowermost centimeters during all sampling season, except July when it was warmer (−0.5 to −1 °C at P5 and P6). In July and August the sea-ice temperature increased within the sea ice to the top centimeters due to warmer air temperatures in these months. Brine salinities differed largely between the seasons and stations depending on ice in situ temperatures. Following the temperature gradient, the calculated brine salinities increased from December to May from bottom to top with highest values of 238 in the top 2.5 cm of sea ice at station P7 in March 2021. In July/August brine salinity was lowest in the warm top centimeters of the ice and only ranged between 0.4 and 31.0. The calculated relative brine volume fraction was during all sampling season >5 % in the 10 lowermost bottom centimeters of the ice (exception P6 in March 2021, <5 %), while on average the fraction was <5 % in the top centimeters of the ice. In most cases, the relative brine volume increased from the top towards the bottom, with large variations in the interiors of the sea-ice cores.

3.2. Seasonal dynamics of integrated Chla, POC, protist biomass and meiofauna abundance/biomass

The Chla:Phaeo ratio was the lowest during March, July and December (Table S3, value ranging between 0.7 and 2.3). In August 2019, the average ratio was 3.3 across stations and the highest value recorded in May 2021 was 8.4 at P4 and 6 at P7. The molar C:N ratio was highest in March (ranging from 17 to 47, Table S3), July and December, and lower in August and May (ranging from 7 to 13, Table S3). Integrated Chla (0–30 cm) showed a clear seasonal pattern (Fig. 3a) with minimum values of <0.2 mg m^{-2} in March and a ~10 to 100-fold increase to peak values of up to 29.4 mg m^{-2} in May. By July and August integrated Chla had declined again (range from 1.1 to 3.2 mg m^{-2}). December integrated Chla at station P5 was similar to values measured in March while it exceeded those measured at station P7 in July and August. In contrast to Chla, integrated POC showed no clear seasonal pattern (Fig. 3b) with average March values (796 ± 229 mg C m^{-2}) being only slightly lower than those measured in May, July and August (1082 ± 433 mg C m^{-2}). POC:Chla ratios were high throughout the year (range from 258 to 23,352, Table S3), except in May when the POC:Chla ratios were <160.

Integrated sea-ice protist biomass also increased drastically from March to May, remained elevated from July through August and differed notably in December (Fig. 3c). Diatoms were dominant taxonomic group in biomass estimates, except in March when flagellates were dominant, and co-dominant with dinoflagellates in August. The seasonal pattern of diatoms followed that of integrated Chla, with highest biomass observed in May while dinoflagellates and flagellates showed a secondary peak in August, similar in magnitude to the one in May. The August peak was particularly pronounced in ciliates, exceeding May biomass by roughly a factor of 2, in agreement with the seasonal trend of larger ciliate biomass and abundance in the meiofauna fraction (Fig. 3d, e). Compared to the other protist groups integrated ciliate biomass was low in December at station P7.

At higher taxonomic resolution (Fig. 4), pennate diatoms dominated integrated diatom biomass throughout the seasons with minor contributions of *Attheya septentrionalis* and some pelagic species belonging to the genus *Thalassiosira* as the dominant centric diatoms (Fig. 4a). In March 2022 *Navicula septentrionalis, Thalassiosira* cf. *gravida/antarctica* and *Nitzschia frigida* dominated diatom biomass while in March 2021 *Navicula* spp. (few *N. transitans*), *Thalassiosira* spp. (including spores) and unidentified pennate diatoms were the dominant taxa. From the peak in May to August, typical pennate sea-ice diatoms including *Navicula pelagica*, *N. transitans*, *Nitzschia frigida*, *Diploneis litoralis* and *Entomoneis paludosa* dominated diatom biomass. The surprisingly high diatom biomass at station P7 in December was dominated by *N. pelagica* (>77 % of total diatom biomass). Taxa belonging to the dinoflagellate order Gymnodiniales including the several unidentified species of the genus Gymnodinium, dominated integrated dinoflagellate biomass throughout the year (Fig. 4b). Other species such as *G. ostenfeldii* dominated integrated biomass during several seasons (March 2022, July and August). *Cochlodinium* spp. were an important part of the dinoflagellate biomass at almost all seasons (but not in December). Within the flagellates, unidentified flagellates (particularly the 7–10 μm size group) dominated integrated biomass with unidentified chrysophytes and the green algae *Pyramimonas* spp. coming next in importance (Fig. 4c). In May ciliate biomass was dominated by the mixotrophic species *Mesodinium rubrum*, particularly at station P6, together with *Strombidium* sp. and *Didinium* sp., except at station P7 where unidentified ciliates and *Euplotes* sp. dominated (Fig. 4d). During peak ciliate biomass in August a mix of *M. rubrum*, *Uronema marinum*, *Didinium* sp., *Strombidium* sp. and unidentified taxa dominated the ciliate community. In March, low ciliate biomass was dominated by *Didinium gargantua* in 2022 and cysts of unidentified ciliates in 2021. In terms of species richness, in May a total of 91 taxa was observed including the highest number of diatom taxa (43), in July 91 total taxa with 29 diatoms, and the highest total number in August with 95 taxa including 33 diatoms.

Overall, the sea-ice meiofauna community was comprised of harpacticoid copepods, different copepod nauplii, rotifers and a diverse range of large ciliates (>20 μm) which contributed significantly to biomass in all seasons. In total we found six different phyla, a list of identified species/taxa and morphotypes is given in the Table S4. The seasonal changes in sea-ice meiofauna biomass (Fig. 3d) followed in general the protist and Chla biomass patterns (Fig. 3b and c). In March 2021 meiofauna was completely absent in 2021 (Q1: P4, P6 and P7), or had very low biomass in March 2022 (on average <0.08 mg C m^{-2}, Fig. 3d). Meiofauna biomass was highest in December (averaged 0.4 mg C m^{-2}), followed by August (averaged 0.3 mg C m^{-2}), excluding a high May value caused by a single amphipod species (P7: 56.71 mg C m^{-2}). Abundances showed a different pattern. Highest abundances were found

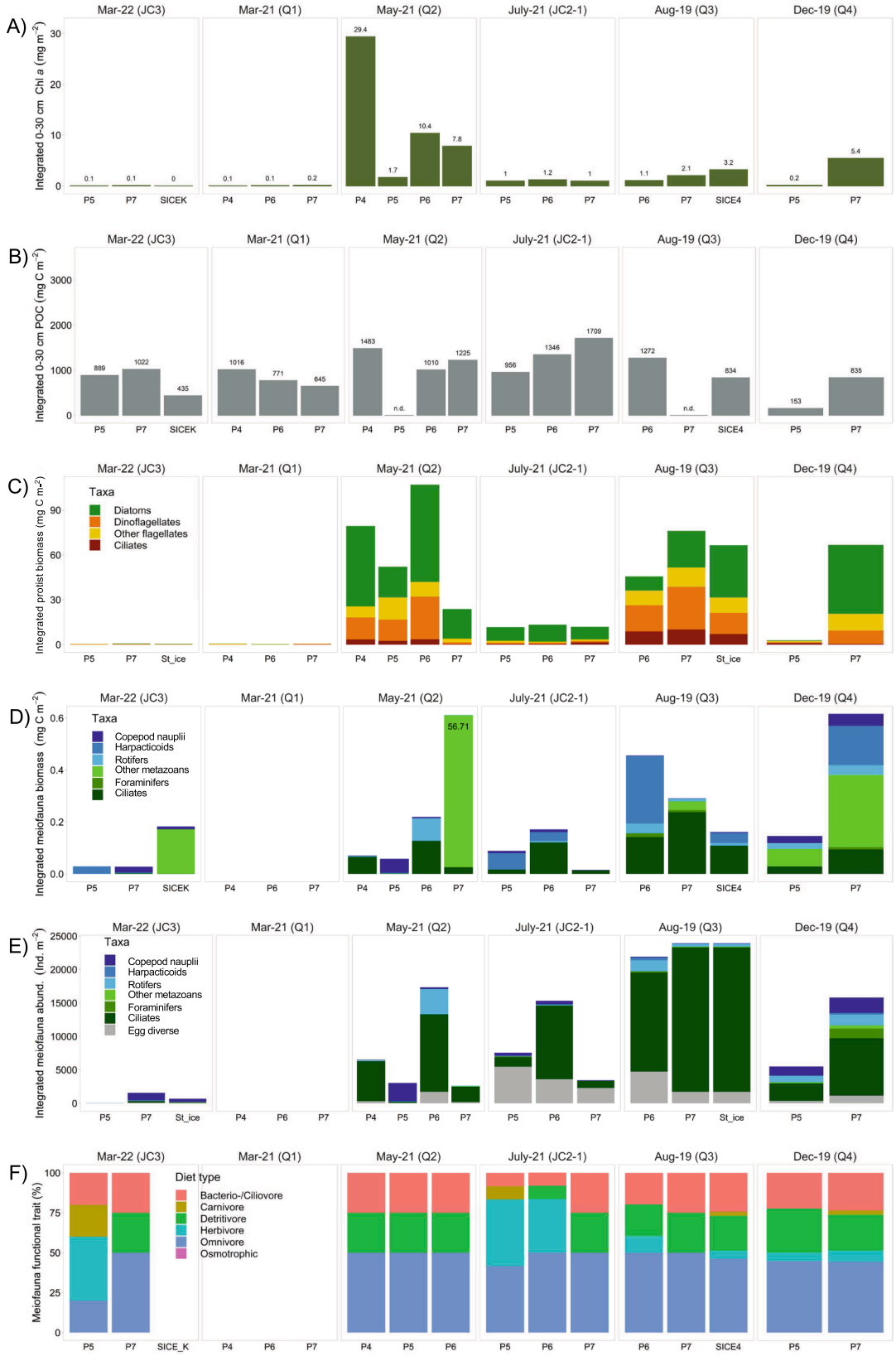

Fig. 3. Depth-integrated A) Chlorophyll *a*, B) POC, C) protist biomass, D) meiofauna biomass, E) meiofauna abundance and F) diet type trait frequency for meiofauna for the lowermost bottom 30 cm of the sea ice. Note the difference on the y-axis for the depth-integrated data. Note at P7 station Q2 sections different scaling for integrated metazoan = 56.71 mg C m^{-2}.

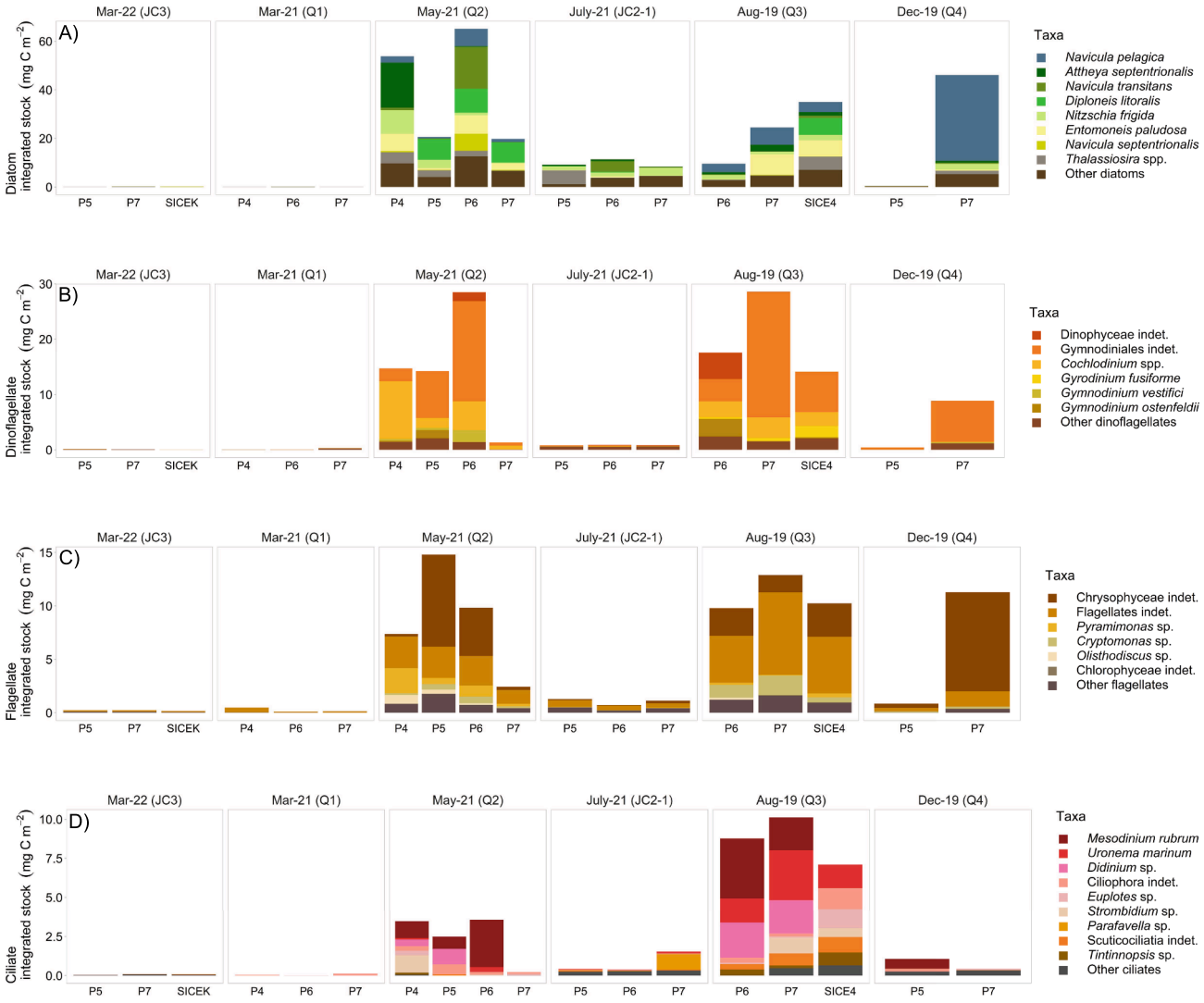

Fig. 4. Depth-integrated biomass (mg C m^{-2}) of the four major protist groups for the lowermost 30 cm of the sea ice: A) diatoms, B) dinoflagellates, C) flagellates and D) ciliates. Note the different y-axis scales.

in August with an average of 23 × 10^3 Ind. m^{-2} (Fig. 3e), and in December with a mean of 11 × 10^3 Ind. m^{-2}. In March (2022), copepod nauplii, harpacticoids, a few ciliates and other metazoans (mainly trochophora larvae at station SICEK) contributed largely to the biomass. In May ciliates dominated the biomass (b) and abundance (a) at P4 (*b*: 0.07 mg C m^{-2}, *a*: 5998 Ind. m^{-2}) and P6 (*b*: 0.1 mg C m^{-2}, *a*: 12 × 10^3 Ind. m^{-2}), while copepod nauplii were a major contributor at P5 (*b*: 0.05 mg C m^{-2}, *a*: 2734 Ind. m^{-2}). The occurrence of a single specimen of the ice amphipod *Apherusa glacialis* caused the high biomass value at P7 (Fig. 3d, b: 56.71 mg C m^{-2}, *a*: 64.8 Ind m^{-2}). We identified at least eleven different morphotypes of ciliates (Table S4), including tintinnids, and the genera *Didinium* spp. and *Euplotes* spp. Rotifers were also common in May, for instance at P6 (*b*: 0.09 mg C m^{-2}, *a*: 3779 Ind m^{-2}), and most rotifers identified belonged to the Order Ploima and about 98 % were assigned to the Synchaetidae family.

Beside high ciliates biomass/abundance, the harpacticoids *Tisbe* spp. and especially *Microsetella* spp. were common in the sea ice at several stations in July and August, (e.g., July at P5: *b*: 0.06 mg C m^{-2}, *a*: 105 Ind m^{-2}). During the phases of high harpacticoid biomass in these summer months, we found many eggs and loose egg sacs in the ice (July: 610–1610 Ind m^{-2}, August: 134–1620 Ind m^{-2}). Many of the eggs were suggested to be copepod eggs. Biomass was not calculated for eggs. Interestingly, we found the planktic foraminifer *Neogloboquadrina pachyderma,* but also benthic foraminifers, such as *Elphidium* cf. *excavatum* and *Bolivinia* spp., both alive and dead in the sea ice in July, August and December (Fig. 3d, e). Foraminifers contributed negligibly to the community biomass in July and August (0.004 mg C m^{-2}) due to their low abundance (55–197 cells m^{-2}) and small size.

Total meiofauna biomass in December was 0.15 mg C m^{-2} at P5 (total integrated abundance: 5494 Ind. m^{-2}), similar compared to May, July and August. P7, however, had the highest biomass (0.62 mg C m^{-2}) from all stations in all seasons and presented a very diverse community composition for that time of the year. Foraminifers were quite common in the ice (1462 Ind. m^{-2}) next to ciliates (8558 Ind. m^{-2}), copepod nauplii (2296 Ind. m^{-2}) and rotifers (1617 Ind. m^{-2}) and they contributed a little more to the biomass (0.009 mg C m^{-2}) than in the summer months. The highest biomass, here, was estimated for other metazoan (0.3 mg C m^{-2}) that belonged to acoels (white morphotype, Phylum Xenacoelopmorpha) and gastropods, potentially the subfamily Lacuninae.

The traits analysis revealed that the meiofauna community was comprised of mainly pelagic species with relatively low salinity and temperature tolerance that were present in the ice year-round (Fig. S5). The frequency of species with varied tolerance did not fluctuate much

with seasons, nor did feeding mode or diet traits (the latter given in Fig. 3f, other in Fig. S5). Omnivores represented the most dominant diet type trait frequency throughout the year (25–50 %, Fig. 3f), followed by detritivores (~25 %) and bacterio-/ciliovores (~25 %), while purely herbivore species only were represented in a smaller fraction in August and December (<15 %), but were dominant in July (~30 %) at P5 and P6, as well as at P5 in March (2022). Suspension feeders were most present in May (Fig. S5).

A Correspondence analysis (CA) and a Constrained Correspondence analysis (CCA) were run with both protist and meiofauna community datasets (Fig. 5, S2.2 for explanatory variables and detailed results). The CCA model was only significant for the protist community (Fig. 5b) but not for the meiofauna community (CA presented in Fig. 5a). As the outcome of the CA for sea-ice meiofauna abundance and biomass was similar and showed little variation, we only present the CA based on abundance here. Further, a Canonical Correspondence Analysis (CCA) was also performed for both protist and meiofauna abundance and biomass data. The CCA model was not significant for the sea-ice meiofauna data and is, therefore, not presented. The CCA model with the protist data was significant for both abundance and biomass, and only the abundance-based CCA results are presented here to keep results comparable with the meiofauna CA.

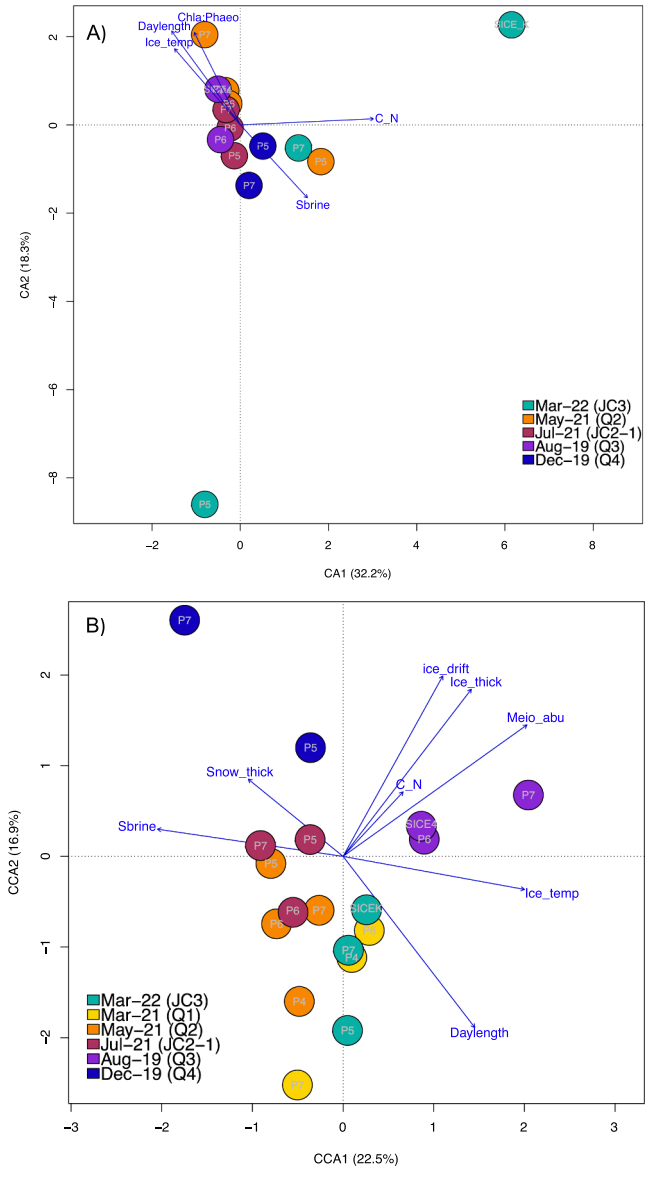

Fig. 5. A) Correspondence Analysis (CA) based on integrated ice meiofauna abundance of large taxa groups. Significant variables ($p < 0.05$) were fitted onto the CA (detailed results in Table S2.2) and B) Canonical Correspondence Analysis (CCA) based on integrated ice protist abundance (Family level). Filled circles indicate station and season sampled. Arrows represent quantitative and standardized explanatory vectors with arrowheads indicating their direction of increase (results in Table S2.2). Explanatory variables/vectors: Chla:Phaeo = Chlorophyll *a*: Phaeophytin ratio, Ice_thick = Ice thickness, Algae_abu = total protist abundance, Snow_thick = Snow thickness, Ice_temp = Ice in situ temperature, Sbrine = Brine salinity, Chla_tot = total Chlorophyll *a* concentration, BrineVol = Brine volume.

The meiofauna samples corresponded very much with each other and hence grouped around the zero point (Fig. 5a), especially the communities in July and August. SICEK and P5 samples in March, however, were ordinated furthest away from the other samples and were most dissimilar. Abiotic and biotic variables were fitted onto the CA but only significant variables ($p < 0.05$) are shown. Variables that influenced the meiofauna community composition to a certain degree in May, July and August were Daylength, Chla:Phaeo ratio and ice temperature, while brine salinity influenced March and December composition. While the CA for the most part did not indicate large variations, the one-way PERMANOVAs test (see S2.3 for details) found significant differences between meiofauna community datasets (integrated abundance presented, biomass results in S2.3) and Month (March, May, July, August, December; $R^2 = 0.74$, $p < 0.0001$) and daylength ($R^2 = 0.6$, $p < 0.004$). Further PERMANOVA tests indicated that meiofauna abundance showed significant differences for the origin of the ice floe (shelf versus basin areas; ($R^2 = 0.19$, $p < 0.02$).

The CCA model ($p < 0.001$) with protist data showed a more distinct seasonal separation than the meiofauna dataset. The CCA1 axis explained 22.5 % ($p < 0.005$) and CCA2 axis 16.9 % ($p < 0.032$) of the variance (total inertia: 32.8, constrained: 21.3, unconstrained: 11.5). March samples of both years grouped together and showed similarities with P6 in July and most of the May stations. Low snow thickness seemed to be a driver (negative correlation) of the protist communities in July (P5, P7) and December (P5, P7). Other significant explanatory variables such as highest meiofauna abundance, highest ice thickness and elapsed time of ice drift were driving the community composition in August. These variables and time of daylength explained the most variation between August versus the other months. Ice temperature, brine salinity and C:N ratio were not significant. The one-way PERMANOVA tests supported the CCA model (see S2.3 for details) and found significant differences between protist community datasets (integrated abundance presented and biomass results in Table S2.3) and Month (March, May, July, August, December; $R^2 = 0.78$, $p < 0.0001$) as well as daylength ($R^2 = 0.6$, $p < 0.0006$). Further tests indicated that there were significant differences between protist communities regarding ice thickness ($R^2 = 0.93$, $p < 0.03$) and elapsed time of ice drift ($R^2 = 0.97$, $p < 0.001$).

3.3. *Vertical distribution patterns of Chla and (POC concentrations, protist and meiofauna abundance/biomass*

Chla was very low but measurable in March of both years, with concentrations ~0.09 μg/L in the lowermost 3 cm and usually decreasing towards the top of the ice (S6 a). Highest ice Chla concentrations were recorded in May in the lowest 3 cm at P4, P6 and P7 with values between 10 and 181 μg/L, with the highest record in the relatively thin ice (22.5 cm) at P4 (Table 1). In July and August, vertical Chla profiles showed average concentrations of 2.4 μg/L in the lowermost ice section. In these two months a different pattern was observed, and Chla concentrations in the ice interior were comparable to or higher than in the lowermost bottom centimeters (e.g., July – P6, August SICE4, S6 a). In December, high concentrations of Chla were measured at P7, (0.4–6.5 μg/L) with the highest values in the 10–20 cm ice section and not the bottom section. At P5 Chla was rather negligible from bottom to top (Chla: <0.1 μg/L) and comparable with March periods.

POC concentrations were relatively homogenous throughout the different seasons (S6 b vertical plot, also see also Fig. 3b) and also vertically, with a much weaker concentration gradient from bottom to top compared with Chla. In March (2021 and 2022), highest POC values were measured in the bottom 10 cm of the ice with an overall station average of 1516 µg/L. Very high values were detected at SICEK with 5030 µg/L in the bottom 3 cm. Highest POC concentrations, agreeing with highest Chla values, were found in May at P4 in the lowermost 3 cm (7907 µg C L^{-1}). In July and August POC varied between 236 and 3120 µg/L, including high POC concentration in the top centimeters at SICE4 in August (150–160 cm: 3120 µg/L). In December, POC was between 336 and 565 µg/L at P5 and varying between 417 and 900 µg/L at P7, thus, in contrast to the Chla pattern, relatively similar with slightly higher concentrations at P7 (10–20 cm: 900 µg/L).

The algae abundance was low in March 2021 and 2022 with maximum abundances of 0.1 × 10^6 cells L^{-1} in the bottom 3 cm (e.g., at Q1 - P7, Fig. 6a), dominated by flagellates. In the top ice section at SICEK and P7 (March 2022) diatoms of the genus *Navicula* spp. *and Nitzschia frigida* were slightly higher in abundance. In March 2022, the vertical protist biomass distribution was higher for dinoflagellates, especially in some sections at P5 and P7, dominated by *Gymnodinium* spp.. Overall, the vertical biomass distribution of protists at most stations followed the abundances pattern (Fig. 6b). In May, highest abundances were recorded in the bottom 3 cm at P4 (30 × 10^6 cells L^{-1}) with diatoms dominating in abundances and biomass and decreasing to the top of the ice (Fig. 6). Also in July, diatoms were the major taxa contributing to abundance (and biomass) within the ice, mainly in the bottom centimeters, but very low in abundances (<2 × 10^6 cells L^{-1}) with *Nitzschia frigida* observed at all stations. In August 2019, unidentified flagellates (3–7 µm) dominated the protist composition in abundance (Fig. 6a). The haptophyte *Phaeocystis pouchetii* (not shown), was also present, but did not contribute much to biomass. The protist biomass was more homogeneous in composition compared to the other months, with co-dominance of diatoms (e.g., *Synedropsis hyperborea, Nitzschia frigida*

Fig. 6. Vertical distribution (lowermost 30 cm of ice floes) of sea-ice protist groups in the different months in the northwestern Barents Sea. A) Abundance (in 10^6 cells L^{-1}), and B) Biomass (µg C L^{-1}) for the four major taxonomic groups. "St_ice" refers to the various SICE stations cruise, see Table 1. Note that the x-axis for the March cruises is different from the others.

and *Navicula pelagica*) and especially dinoflagellates (e.g. Dinophyceae indet., Gymnodiniales indet., *Cochlodinium* sp.). Ciliates such as *Mesodinium rubrum, Didinium* sp., and *Uronema marinum* among others, were low in abundance but contributed a higher biomass share. In August, the abundance and biomass were not concentrated in the bottom 3 cm of the ice, but also found to be stable in the other sections compared to the other sampling periods. Protist abundance at P5 in December was low throughout the whole core supporting the Chla results (Fig. S6a). At P7, as the Chla and POC results indicated (Fig. S6), the protist community was dominated by diatoms in abundance and biomass throughout all ice sections (e.g., at 3–10 cm, a: 2.2 × 10^6 cells L^{-1}, b: 250 µg C L^{-1}) followed by unidentified flagellates (3–7 µm) and within high abundance of Chrysophyceae cysts (e.g., at upper ice sections, 0.5 × 10^6 cells L^{-1}).

In March, sea-ice meiofauna was either completely absent (2021) or occurred in very low in abundance in the lowermost three centimeters (e.g., 23 Ind. L^{-1} at P7 in 2022), with decreasing abundance higher up in the ice (Fig. 7a). In May, abundance and biomass were also highest in the bottom 3 cm, with very few animals found higher up in the ice column. Highest abundance (0–3 cm: 837 Ind. L^{-1}) was detected at P6, dominated by rotifers (132 Ind L^{-1}) and ciliates (0–3 cm: 651 Ind L^{-1}). Biomass was highest in the lowermost centimeters of P7 (2.1 µg C L^{-1}), explained by a single *Apherusa glacialis* specimen (see above). Meiofauna abundance was more uniformly distributed within the four core sections in July (e.g. P6: 44–62 Ind L^{-1}) with a slightly higher variability in

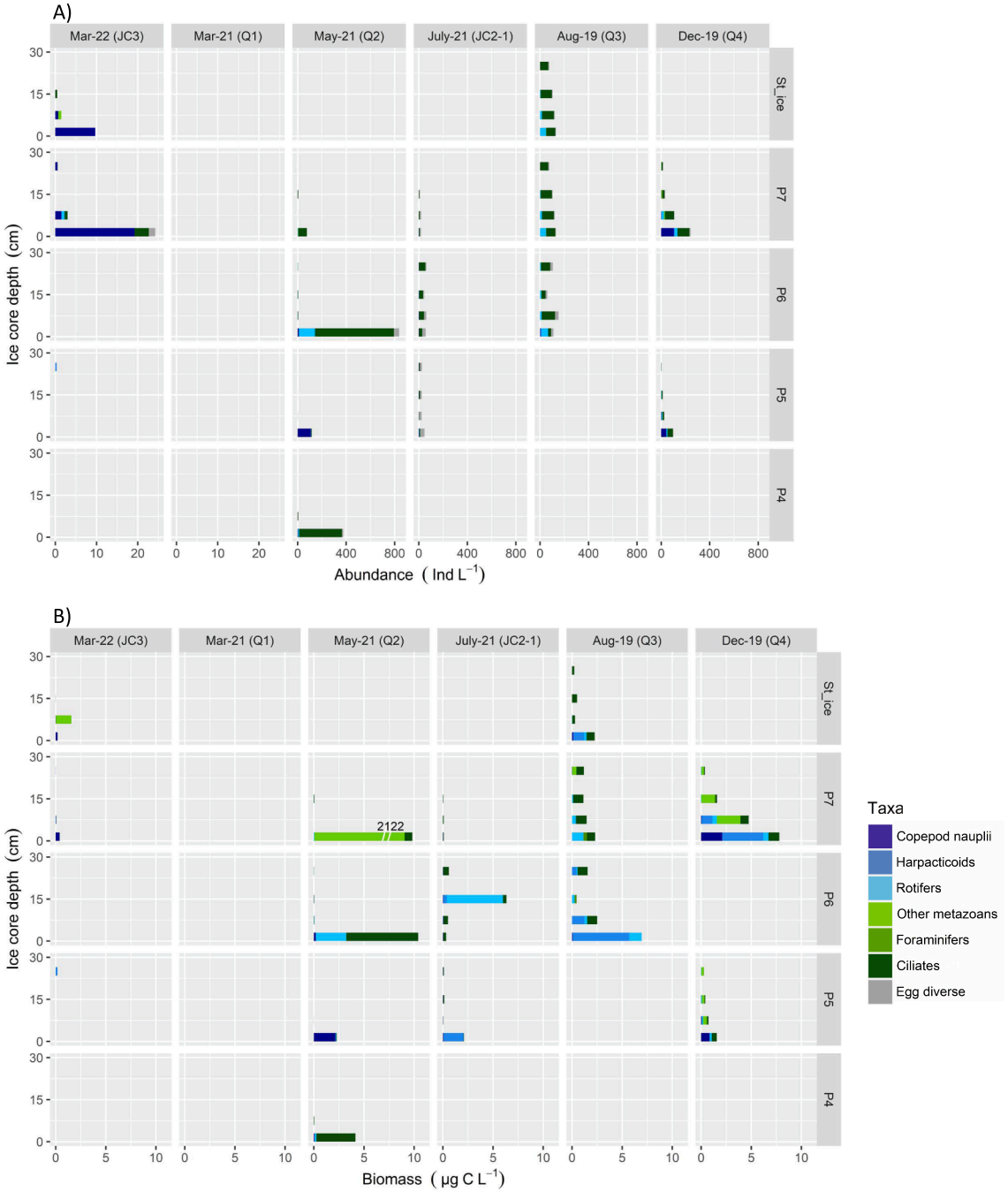

Fig. 7. Vertical distribution (up to 30 cm) of sea-ice meiofauna, including large ciliates and metazoan eggs, through the different months in the northwestern Barents Sea. A) Abundance (Individuals L^{-1}) for the major taxa and eggs counted. B) Biomass estimates (µg C L^{-1}), eggs are not included here. Stations indicated on the right side, "St_ice" standing for the different SICE stations per cruise, see Table 1. Note the x-axis can vary in the different months.

biomass. For instance, at P6 biomass peaked in the 10–20 cm section (0.006 μg C L^{-1}, Fig. 7b), mainly driven by rotifers. In August ciliates were the main contributors throughout all ice sections examined with little vertical variability (Fig. 7). Similar to July, biomass was more variable and highest in the lowermost 3 cm and peaked at P6 (7.0 μg C L^{-1}) with harpacticoids as main contributor (5.6 μg C L^{-1}). In December, similar abundances were found as in August (~100 Ind L^{-1}). However, in this month the values were highest in the bottom 3 cm and decreased towards the higher sections, with P7 highest in abundance (0–3 cm: 243 Ind L^{-1}) and biomass (8 μg C L^{-1}). Abundance and biomass were lower at P5 in December (a: 3.6–101 Ind L^{-1}, b: 0.3–1.5 μg C L^{-1}) but showed the same decreasing trend from bottom to top.

4. Discussion

This study is, to our knowledge, the first seasonal investigation characterizing both sea-ice primary and secondary producers over the entire seasonal cycle in the northwestern Barents Sea. Although the samples were taken as a series of snapshots in non-contiguous years due to the unfortunate worldwide COVID-19 pandemic, they depicted clear seasonal signals of biological responses (Fig. 3) to the changing environment (Fig. 5). Sea-ice protists and meiofauna were found all year round in varying abundances and biomass (apart from meiofauna in March 2021). The seasonal succession pattern was especially pronounced in the sea-ice protist community and algal biomass, while meiofauna showed a delayed response relative to the protists and not much variation in composition. In addition, many of the meiofauna taxa identified in this study can switch between summer grazing and winter omnivory (Marshall, 1949; Uye et al., 2002; Kramer, 2011) leading to less pronounced seasonal changes in feeding trait composition. To develop a seasonally-based scenario, we therefore defined seasons according to ice algal phenology as March – late winter/early spring, May – (late) spring, July – late-bloom/early summer, August – late summer/autumn and December – polar night/winter.

4.1. March – late winter/early spring

In March (2021 and 2022) Chla, protist and meiofauna biomass was negligible or even absent. Diatom biomass values (0.25–0.27 mg C m^{-2}) were similar to data from sea ice in northwestern Svalbard in March to May (Leu et al., 2015 and references therein) but higher than in the Nansen Basin in March (Olsen et al., 2017; Granskog et al., 2018). The high POC values in March, coupled with concurrently low algal and meiofauna biomass, suggest the presence of other carbon fractions not examined in our study, such as detritus, viruses, bacteria, and exopolymeric substances. These components may occur in sea ice in high proportions and dominate during wintertime (Krembs et al., 2011; Torstensson et al., 2023). High C:N ratios well above the Redfield ratio of 6.6 in both March 2021 (C:N = 18) and 2022 (C:N = 32) suggested allochthonous sources of carbon.

The sea-ice diatom composition in the two March periods was largely similar (Fig. 5b CCA) and somewhat diverse with dominance of, e.g., *Navicula septentrionalis, Thalassiosira* spp. and *Nitzschia frigida*. We only detected small differences: the community composition comprised more pelagic species in 2021 while in 2022 the ice-associated diatom *Nitzschia frigida* was more abundant. In both years, the occurrence of pelagic diatom taxa belonging to the genus *Thalassiosira* suggests recruitment from the water column. *Thalassiosira* is a very common pelagic genus in Arctic seas (Poulin et al., 2011) and more frequently observed in FYI compared to older ice (Hop et al., 2020). These March findings were overall consistent with earlier findings that early spring sea-ice communities are usually diverse during the early stage of freeze-up, which later will evolve towards a more typical sea-ice assemblage (Kauko et al., 2018).

At first sight, the low densities of biota during March may be explained by the overall high brine salinity and low brine volume fraction which may inhibit the presence of sea-ice biota specifically in impermeable ice interior sections (Friedrich, 1997; Golden et al., 1998, 2007). This is for example also suggested by the low tolerance to extreme environmental settings found in the meiofauna trait analysis (see Fig. S5c and d). However, the bottom 10 cm of the sea ice did not actually show extreme values for physical properties and, still, meiofauna was genuinely low in abundance (2022) or even absent (2021). This finding could be related to a lack of seeding from the water column, sea floor or other ice floes, or it points towards the importance of water depth. Specifically benthic-origin taxa were limited in their occurrences to shallow shelf stations where recruitment from the benthos might have been facilitated as evident in the 2021 samples (Carey and Montagna, 1982; Gradinger et al., 1999; Arndt et al., 2009). This argument is also supported by the higher abundance of pennate diatoms in March 2022, as those may survive in surface sediments and are brought back to the surface water layers by mixing processes from where they can enter sea ice (von Quillfeldt et al., 2003). Despite that, the low abundance of ice algae and other protists made food availability a likely limiting factor for meiofauna in March. Despite the food scarcity, copepod nauplii (i.e., young developmental stages) were the major group found in the Barents Sea ice in March (2022), albeit in very low abundance (e.g., P7 with <20 Ind. L^{-1}). This finding is consistent with an earlier study from south of Svalbard/Storfjorden in March (up to 100 Ind. L^{-1}) (Schünemann and Werner 2005). Schünemann and Werner (2005), and references within, concluded that the copepod nauplii may endure the food-limited winter in the pack ice by being non-feeding naupliar stages or living of their storage lipids. Some even younger stages, namely metazoan eggs, were also present in the brine channels as early as March. Those potentially belonged to the copepods *Calanus hyperboreus* and/or *Oithona* spp.. Eggs of the winter spawner *C. hyperboreus* were present in the water column during our cruises in December and March. The wax-ester rich eggs are buoyant and drift to the under-ice surface ready for spawning in March to April for the nauplii to be able to graze on sea-ice algae (Conover et al., 1991). This explains their winter occurrence in our sea ice samples. In contrast the life cycle of *Oithona* spp. is not tied to the spring bloom, and therefore eggs were found during all sampled seasons (pers. observations by Christine Gawinski, UiT The Arctic University of Norway).

Similar ice characteristics contributed to the limited interannual variation in community structure of ice biota between March 2021 and 2022. In both years potentially locally formed and young, first-year ice dominated, which limits the time for sea-ice biota recruitment and seeding (Niemi et al., 2011; Kiko et al., 2017; Kauko et al., 2018).

4.2. May – (late) spring

From March to May, ice biota abundance and biomass strongly increased and community composition shifted for both protists and meiofauna in the young first-year ice. This is in agreement with earlier studies on protists in the winter to spring bloom transitions (Niemi et al., 2011; Olsen et al., 2017; Hegseth and von Quillfeldt, 2022). Evidence for reaching the spring bloom stage was our integrated algal biomass values exceeding 1 mg Chla m^{-2}, which Leu et al. (2015) suggested as the threshold for defining an ice algae spring bloom. Our estimations for Chla and protist abundance in May were comparable to but lower than reported earlier in May for Barents Sea pack ice (Hegseth and von Quillfeldt, 2022). Abundance differences among stations could be related to local episodic ice melt events, e.g., at station P5 where also bulk salinity was relatively low, potentially due to melt events. Interestingly, high Chla biomass at station P4 was not reflected in the microscopy-based protist biomass estimates which could be caused by loss of algae during sampling, or high contributions of small protist size classes (Müller et al., unpublished) which are hard to detect by light microscopy.

In May protist community composition reflected a typical (late) sea-ice spring bloom situation: ice algae were dominated by pennate

diatoms such as *Nitzschia frigida* and *Navicula pelagica*, while centric diatoms such as *Thalassiosira* spp. and *Attheya septentrionalis* occurred in lower abundances as found in earlier studies (Tamelander et al., 2009; von Quillfeldt, 2000; Poulin et al., 2011; Arrigo, 2014; Hop et al., 2020). Other typically ice-associated pennate taxa previously recorded in the Barents Sea were *Diploneis litoralis* and *Entomoneis paludosa* (Poulin and Cardinal, 1982; Ratkova and Wassmann, 2005). Furthermore, the highest recorded Chla:Phaeo ratio of 2–8 and low C:N ratio (7–11) close to Redfield ratio (Redfield et al., 1963) indicated growing and generally not nutrient limited sea-ice algae (Gosselin et al., 1990; Gradinger, 2009). Yet, differences in snow cover and resulting different irradiances and algal growth kinetics could have caused to local minor nutrient limitation or delayed algal growth effects indicated by highest C:N recorded at highest snow cover (Tables 1 and S3).

In May, sea-ice protists and meiofauna contributed most to total POC, similar to May observations from north of Svalbard (Fernández-Méndez et al., 2018). The POC:Chla ratio range of 50–156 was comparable to earlier values for ice algae in the Canadian Arctic (15 – 180, Hudson Bay, Gosselin et al., 1990). However, the upper values in either study were higher than the typical value found in healthy algal cells (45, Passow, 1991) again, as in March, pointing towards other particulate carbon sources existing within the ice not determined here (Torstensson et al., 2023).

Similar to March, highest meiofauna and protist abundances were found in the lowermost bottom centimeters as is typical in growing first-year ice (Gradinger et al., 1999). The large contribution of larger ciliates and metazoan eggs are in line with previous sea ice spring studies (Nozais et al., 2001; Marquardt et al., 2011; Ehrlich et al., 2021). Also, harpacticoid copepods (Melnikov, 1989; Werner, 2005; Hirche and Kosobokova, 2011; Kosobokova et al., 2012, Timchenko et al., 2021) and rotifers are commonly reported from the ice habitats (Friedrich 1997; Friedrich and De Smet, 2000). Averaged integrated metazoan abundances from all four stations varied between 130 and 4038 Ind. m^{-2} which was slightly lower than values in Timchenko et al. (2021) who studied sea ice in April–May 2019 very close to our stations. Backtracking exercises in both Timchenko et al. (2021) and the present study indicated ice origin north of Franz Josef Land. Yet Timchenko et al. (2021) found benthic taxa in their samples, albeit in low abundance, including Acari and Nematoda, which were absent in our study. They reported high abundances of harpacticoids, calanoid copepods and amphipods, but noted the absence of rotifers. Differences could be attributed to the extreme heterogeneity of the sea ice habitat down to the small scale (Spindler, 1994).

The absence of nematodes throughout all seasons and stations in this study has also been found in other recent studies (Ehrlich et al., 2021; N-ICE dataset in Bluhm et al., 2018), and is potentially caused by a fundamental change in the sea ice regime. Nematodes, platyhelminth flatworms and acoels, the latter only found at a single occasion in December in this study, have previously reported as the most abundant taxa in several Arctic sea-ice studies (Friedrich, 1997; Gradinger, 1999; Gradinger et al., 1999; Nozais et al., 2001; Schünemann and Werner, 2005; Gradinger et al., 2005). Nematodes are assumed to colonize the sea ice from sediments in shallow waters (Carey and Montagna, 1982; Gradinger et al., 1999) and even reproduce in the ice (Marquardt et al., 2011; Gradinger and Bluhm, 2020; Ehrlich et al., 2021). Ehrlich et al. (2021) hypothesized that the absence of nematodes may reflect the reduction in multi-year ice and a reduced connectivity between the ice-producing Siberian shelves and the pack-ice areas of the deep Arctic Basin suggested by Krumpen et al. (2019). Further, the transition from a multi-year to a predominant seasonal Arctic ice cover limits the time for completing life cycles in the sea ice and will benefit biota of pelagic origin (Kiko et al., 2017; Ehrlich et al., 2021). This conclusion is generally supported by our results and by the substantial compositional overlap of the ice meiofauna with the under-ice community, which was only qualitatively sampled (Marquardt et al., 2023f).

4.3. July – late-bloom/early summer

By July, the main spring bloom had terminated and a more heterotrophic and detritus dominated succession stage was reached. Evidence for this interpretation lies in algal biomass values in the lowermost ice sections being below the spring bloom threshold of 1 mg Chla m^{-2} (Leu et al., 2015), as well as lower algal abundances, higher POC:Chla and C:N ratios and high abundance of large ciliates in the meiofauna community. The more heterotrophic succession stage of ice biota in July combined with older ice ages (old FYI or SYI) could explain the higher POC concentration in our study (1100–1438 mg POC m^{-2}) compared to data from FYI east of Svalbard (543–620 mg POC m^{-2} in Tamelander et al., 2009) as the older ice might have retained organic matter through the melt seasons.

The low protist biomass in July was still dominated by diatoms. Species typical for the end of spring in the Barents Sea (e.g., Tamelander et al., 2009) were found such as the sea-ice diatoms *Navicula transitans* and *Nitzschia frigida* and pelagic species of the genus *Thalassiosira* (Leu et al., 2015). Interestingly, increased Chla values were found higher up in the ice which can be explained through more accessible interior space by higher internal permeability of summer sea ice (Tedesco et al., 2019) combined with biomass loss at the ice bottom due to melt (Gradinger et al., 1991; Assmy et al., 2013; Boetius et al., 2013). The high meiofauna abundance in July could also have contributed towards the decrease in ice algal biomass through grazing (Werner, 1997; Michel et al., 2002), as also supported through the trait frequency of herbivores (e.g., at P5 and P6).

Interestingly, eggs were the most abundant contribution to total meiofauna abundances at this time with 54 %. The high abundance of eggs and their presence in all seasons in this and earlier studies (Carey, 1992; Friedrich, 1997; Marquardt et al., 2011; Ehrlich et al., 2021) highlights once again the importance of sea ice as a nursery and reproduction ground (Grainger et al., 1985; Søreide et al. 2010; Marquardt et al., 2011). This habitat function will likely be impacted by progressive sea ice loss.

Metazoan abundance was relatively low compared to previous studies in the Arctic during June-July (Beaufort Sea - Kern and Carey (1983); North of Svalbard – Ehrlich et al., 2020; Barrow Alaska - Gradinger et al., 2010). Such low values were unexpected given we sampled old FYI/SYI, which would have had longer time for settlement and growth of allochthonous ice metazoans than the sea ice that we sampled earlier in the year. Here a combination of several factors may be the cause, including the lack of multiyear ice (MYI) providing seed populations of ice-endemic taxa, and the great water depth limiting the presence of often highly abundant larval and juvenile stages of benthic taxa in sea ice of shallow seas (Bluhm et al., 2017). Large ciliates contributed substantially to meiofauna abundance in our study in July, consistent with earlier studies (Gradinger et al., 1991; Marquardt et al., 2011; Ehrlich et al., 2020). Ciliates dominating within the ice habitat may be explained through faster reproduction by cell division than metazoans. Their high relative contribution combined with the unique species composition of Arctic ice ciliates which is distinctly different to pelagic communities (e.g., Agatha et al., 1993) warrants a more detailed study on their biodiversity in future research.

Although low in abundance, foraminifers including the pelagic *Neogloboquadrina pachyderma* and a few unidentified benthic specimens were found alive at two stations (P5 and P6). *N. pachyderma* is the dominant pelagic foraminifer species in polar regions (Volkmann, 2000; Schiebel and Hemleben, 2017) including the Barents Sea (Anglada-Ortiz et al., 2023). It has, however, only been sporadically observed within Arctic sea ice (Bluhm et al., 2018 and references therein), while regularly occurring in Antarctic ice (Dieckmann et al., 1991). Finding this species in Barents Sea ice is not only biologically interesting but also relevant for paleoenvironmental applications (Bertlich et al., 2021). Supporting the passive transport theory, it is noteworthy that we detected not only living but also dead (transparent) individuals of

N. pachyderma at all stations in very high numbers (Table S4). Incorporation of this pelagic species could have happened while drifting over the deep basin water. In contrast, sea ice sampled in July drifted all the way from the Kara Sea (Fig. 2d) on the shallow Siberian shelf (on average ~130 m, Jakobsson, 2002). This origin could explain the presence of benthic foraminifers within the sea ice.

4.4. August – late summer/autumn

Ice algal biomass in August was slightly higher than in July and comparable to previous studies from the northern Barents Sea (Gradinger and Zhang, 1997) and central Arctic Ocean (Fernández-Méndez et al., 2014) during the same season. The increased protist biomass was dominated by dinoflagellates which cope better with limiting nutrient concentrations typical for this period and are less prone to ablation due to their motility compared to ice-attached diatoms (Horner and Schrader, 1982; Alou-Font et al., 2013; Leu et al., 2015 and references within).

This dominance by heterotrophic taxa (dinoflagellates and ciliates) compared to all other seasons is typical of late summer sea-ice algae community composition (Leu et al., 2015). Similar to July, protist abundance and biomass was low in the lowermost 3 cm, but increased higher up in the core, probably introduced by warmer under-ice water temperature and ice melting (Gradinger et al., 1991; Hegseth and von Quillfeldt, 2022).

In August, we observed the haptophyte *Phaeocystis pouchetii* at all ice sections and stations, and even in high abundances at P7 where it was also highly abundant underneath the ice (Assmy et al. 2022e) and contributed to the vertical carbon flux (Bodur et al., 2023). This microalga is not common in sea ice but can occasionally occur in the brine channels during pronounced under-ice blooms potential initiated by leads in the pack ice (Assmy et al., 2017) and often occurs at later successional stage after the spring bloom in the Barents Sea water column (von Quillfeldt, 2000; Hegseth et al., 2019; Assmy et al., 2022e).

Meiofauna abundance was highest in August for the entire study period and animals were more evenly distributed within the cores than in other seasons. While meiofauna abundances were similar to other Arctic studies, the composition was distinctly different (Gradinger et al., 2005; Schünemann and Werner, 2005; Bluhm et al., 2018). The dominance of ciliates had further increased, followed in abundance by rotifers, which have been previously reported from the Barents Sea (Friedrich, 1997; Friedrich and de Smet, 2000) in similar abundances. Interestingly, again foraminifers were found including *Bolivinia* spp. and *Elphidium* cf. *excavatum.* The latter species is common in sediments of Arctic shelf areas (e.g., Siberian shelf, Bauch et al., 2004) and was also present in Barents Sea sediments during our field campaign (Thaise de Freitas, University of Oslo, pers. observation). Benthic foraminifers are important proxies for the reconstruction of past sea-ice extent due to their fast response to changing environmental conditions (Seidenkrantz, 2013; Fossile et al., 2020). As for July, the sea ice drift trajectories suggest that those benthic foraminifers were incorporated into the sea ice on the shallow Siberian shelf, in this case the Laptev Sea shelf where they have also been reported before (Lukina, 2001; Bauch et al., 2004). We exclude local incorporation at P6 and P7 due to the water depths exceeding 800 m. The occurrence of living specimens within the ice after 400–600 days of drift indicates that they can use the ice as a habitat and reproduce, since their life span may last for up two or more years at higher latitudes (Goldstein, 1999).

4.5. December – polar night/winter

The harsh environmental conditions within Arctic winter sea ice in terms of low irradiance, temperatures, and brine volume fractions and high brine salinities cause substantial stress on biota living within the ice (Lund-Hansen et al., 2020). This agrees with low Chla and protist biomass at P5 as seen in earlier observations (Gradinger and Ikävalko, 1998; Lund-Hansen et al., 2020), pointing towards the heterotrophic phase of the ice biota seasonal cycle (Leu et al., 2015). Surprisingly, the basin-station P7, in contrast, had very high integrated Chla and diatom biomass contributions by phytoplankton species (e.g., *N. pelagica*) frequently observed in the region around Svalbard all year round (Hop et al., 2020). Algal abundances at P7 were even two orders of magnitude higher than winter reports from other Arctic sea ice areas (Beaufort sea – Niemi et al., 2011; North of Svalbard, 2.4×10^6 cells L^{-1}, Hegseth and von Quillfeldt, 2022). This observation supports recent studies that revoked the assumed dormant state of the Arctic ecosystem during the polar night (Berge et al., 2020 and references within).

Long microalgal survival (Johnsen et al., 2020) combined with efficient incorporation of protists into growing sea ice (Gradinger and Ikävalko 1998) can explain this astonishing observation. Microalgae can survive extended periods of time under cold and dark conditions (Niemi et al., 2011; Vader et al., 2015; Hegseth and von Quillfeldt, 2022 and references within). However, we know very little about winter survival at the species level and how that impacts community composition in the subsequent spring. Cysts formed by Chrysophyceae and dinoflagellates, that were also present in this study, have been reported from sea ice before and are a common life cycle strategy to survive the harsh Arctic winter conditions (Stoecker et al., 1998; Montresor et al., 2003; Olsen et al., 2017; Kauko et al., 2018; Hegseth and von Quillfeldt, 2022).

The surprisingly high protist biomass, combined with high POC concentrations, for the season, provided a strong food base for a diverse and highly abundant sea meiofauna community. Again, ciliates dominated, but specifically copepod nauplii were the most abundant metazoans, likely originating from reproduction of pelagic copepods (discussed in 4.1 March). Acoela and gastropod larvae, commonly found in other studies (Gradinger, 1999; Nozais et al., 2001; Gradinger et al., 2005), were only encountered in December. The strong differences between the shelf station P5 and the slope station P7 can be linked to different source populations and age of the ice. P5 station being a very young locally formed ice regime, while the older ice around P7 originated from the Nansen Basin supporting recruitment of ice biota nearby (Olsen et al., 2017).

5. Summary and conclusion

The data demonstrated a strong and partly unexpected seasonality in sea-ice biota. Changes in the timing of ice formation and melt (Lind et al., 2018, Lundesgaard et al., 2022), as well as overall changes in ice transport (Krumpen et al., 2019) will significantly impact composition and phenology of sympagic communities. As expected, seasonality was particularly pronounced in sea-ice algae with typical ice-associated diatoms dominating in spring. Unexpected was the muted seasonality of POC biomass suggesting the sea ice as organic carbon reservoir beyond the productive season. The surprisingly high December abundances, however, further strengthened the recently emerging notion of an active biota in the dark Arctic winter, at least in the Atlantic inflow region while at the same time providing the seed populations for subsequent spring and summer growth. Our findings emphasize the need to strengthen knowledge on activity and biodiversity during the polar night. Ice trajectories and trait studies helped to potentially identify origin and recruitment histories (e.g., of benthic foraminifers) of ice biota and refine how community trait frequencies fluctuate over the year. Here, we recommend help of molecular tools to strengthen the taxonomic resolution (as used by Hardge et al., 2017; Marquardt et al., 2018). The ice meiofauna community was dominated by pelagic taxa (e.g. ciliates, copepod nauplii, rotifers) during all seasons. Especially taxa with shorter establishment times such as ciliates will be favored over benthic-sympagic species (e.g., nematodes). This is furthermore supporting the concept that the loss of older ice types favor pelagic-sympagic species (Kiko et al., 2017; Ehrlich et al., 2020) which may alter the ice-associated carbon pathways (tracked by Ehrlich et al., 2021; Cautain et al., 2022; Kohlbach et al., 2023). Several novel findings in

this study like high winter abundances, the occurrence of foraminifers and the strong ciliate contribution to meiofauna abundance and biomass emphasize the need to study the role of sea ice in the Barents Sea and other Arctic Seas' ecosystems.

Declaration of Competing Interest

The authors declare that they have no known competing financial interests or personal relationships that could have appeared to influence the work reported in this paper.

Data availability

Most data presented in this study are already published as datasets, or are in the phase to be published in the near future.

Acknowledgements

We would like to thank the fantastic captain and crew of R/V Kronprins Haakon who supported our fieldwork. Further, we appreciated the support of all Nansen Legacy chief scientists and the ice teams and polar bear guards that joined us during 2019-2022, special thanks go to Snorre Flo (UNIS), Karoline Saubrekka (UiO), Cheshtaa Chitkara (UNIS), Anette Wold (NPI), Simon H. Kline (UiO), Vanessa Pitusi (UNIS/UiT), Adam Steer (NPI) and Elisabeth Jones (IMR) who on several occasions were supporting ice core handling and postprocessing onboard. We would like to thank Anna Vader (UNIS), Oliver Müller (UiB), Griselda Anglada-Ortiz (UiT) and Thaise Ricardo de Freitas (UiO) for support in field and making data available for this study as well as Teena Chauhan (UiB) for help with identifying benthic foraminifers. Special thanks to Yasemin Bodur (UiT) who was a great help in the field but also in the office with statistical advice and Fig. 1. Lastly, we would like to thank the two anonymous reviewers for their kind words and constructive suggestions. This study was funded by the Research Council of Norway through the project The Nansen Legacy (RCN # 276730).

Appendix A. Supplementary material

Supplementary data to support this article can be found online at https://doi.org/10.1016/j.pocean.2023.103128.

References

Aaboe, S., Lind, S., Hendricks, S., Down, E., Lavergne, T., Ricker, R., 2021. Sea-ice and ocean conditions surprisingly normal in the Svalbard-Barents Sea region after large sea-ice inflows in 2019. In: Copernicus Marine Service Ocean State Report, Issue 5, Journal of Operational *Oceanography*, 14:sup1, s140–s148. doi: 10.1080/1755876X.2021.1946240.

Agatha, S., Spindler, M., Wilbert, N., 1993. Ciliated Protozoa (Ciliophora) from Arctic sea ice. Acta Protozool. 32, 261–268.

Ainley, D.G., Tynan, C.T., Stirling, S., 2003. Sea ice: A critical habitat for polar marine mammals and birds. In: Thomas, D.N., Dieckmann, G.S. (Eds.), Sea Ice: An Introduction to its Physics. Chemistry, Biology and Geology, Blackwell Publishing, Oxford, UK, pp. 240–267.

Alou-Font, E., Mundy, C.-J., Roy, S., Gosselin, M., Agustí, S., 2013. Snow cover affects ice algal pigment composition in the coastal Arctic Ocean during spring. Mar. Ecol. Prog. Ser. 474, 89–104. https://doi.org/10.3354/meps10107.

Anglada-Ortiz, G., Meilland, J., Ziveri, P., Chierici, M., Fransson, A., Jones, E., Rasmussen, T.L., 2023. Seasonality of marine calcifiers in the northern Barents Sea: Spatiotemporal distribution of planktic foraminifers and shelled pteropods and their contribution to carbon dynamics. Prog. Oceanogr. 103121 https://doi.org/10.1016/j.pocean.2023.103121.

Ardyna, M., Mundy, C.J., Mayot, N., Matthes, L.C., Oziel, L., Horvat, C., Leu, E., Assmy, P., Hill, V., Matrai, P.A., Gale, M., Melnikov, I.A., Arrigo, K.R., 2020. Under-ice phytoplankton blooms: Shedding light on the "invisible" part of Arctic primary production. Front. Mar. Sci. 7, 608032 https://doi.org/10.3389/fmars.2020.608032.

Arndt, C.E., Gulliksen, B., Lønne, O.J., Berge, J., 2009. Sea ice fauna. In: Johnsen, G., Kovacs, K., Sakshaug, E. (Eds.), Ecosystem Barens Sea. Tapir Academix Press, Trondheim, pp. 303–314.

Arndt, C.E., Swadling, K.M., 2006. Crustacea in Arctic and Antarctic sea ice: Distribution, diet and life history strategies. Adv. Mar. Biol. 51, 197–315. https://doi.org/10.1016/S0065-2881(06)51004-1.

Arrigo, K.R., et al., 2012. Massive Phytoplankton Blooms Under Arctic Sea Ice. Science 336, 1408. https://doi.org/10.1126/science.1215065.

Arrigo, K.R., 2014. Sea ice ecosystems. Ann. Rev. Mar. Sci. 6, 439–467. https://doi.org/10.1146/annurev-marine-010213-135103.

Arrigo, K.R., Sullivan, C.W., 1992. The influence of salinity and temperature covariation on the photophysiological characteristics of Antarctic sea ice microalgae. J. Phycol. 28, 746–756. https://doi.org/10.1111/j.0022-3646.1992.00746.x.

Arrigo, K.R., 2016. Sea ice as a habitat for primary producers. In: Thomas, D.N. (Ed.), Sea Ice, Third Edition, Wiley Online Library. doi: 10.1002/9781118778371.

Årthun, M., Eldevik, T., Smedsrud, L.H., Skagseth, Ø., Ingvaldsen, R.B., 2012. Quantifying the Influence of Atlantic Heat on Barents Sea Ice Variability and Retreat. J. Clim. 25 (13), 4736–4743. https://doi.org/10.1175/JCLI-D-11-00466.1.

Asbjørnsen, H., Årthun, M., Skagseth, Ø., Eldevik, T., 2020. Mechanisms underlying recent Arctic atlantification. Geophys. Res. Lett. 47 (15) https://doi.org/10.1029/2020GL088036.

Assmy, P., et al., 2013. Floating ice-algal aggregates below melting Arctic sea ice. PLoS One 8 (10). https://doi.org/10.1371/journal.pone.0076599.

Assmy, P., Gradinger, R., Edvardsen, B., Wold, A., Goraguer, L., Wiktor, J., & Tatarek, A., 2022a. Ice Algae Biodiversity Nansen Legacy Q3 [Data set]. Norwegian Polar Institute. doi: 10.21334/npolar.2022.52caaaf1.

Assmy, P., Gradinger, R., Edvardsen, B., Wold, A., Goraguer, L., Wiktor, J., & Tatarek, A., 2022b. Ice algae biodiversity Nansen Legacy Q4 [Data set]. Norwegian Polar Institute. doi: 10.21334/npolar.2022.a5059ae6.

Assmy, P., Gradinger, R., Edvardsen, B., Wold, A., Goraguer, L., Wiktor, J., Tatarek, A., & Smola, Z., 2022c. Ice algae biodiversity Nansen Legacy Q1 [Data set]. Norwegian Polar Institute. doi: 10.21334/npolar.2022.b7dc0d05.

Assmy, P., Gradinger, R., Edvardsen, B., Goraguer, L., Wiktor, J., Tatarek, A., & Smola, Z., 2022d. Ice algae biodiversity Nansen Legacy JC2-1 [Data set]. Norwegian Polar Institute.

Assmy, P., Gradinger, R., Edvardsen, B., Wold, A., Goraguer, L., Wiktor, J., Tatarek, A., Dąbrowska, A.M., 2022e. Phytoplankton biodiversity Nansen Legacy Q3 [Data set]. Norwegian Polar Institute. doi: 10.21334/npolar.2022.dadccf78.

Assmy, P., et al., unpublished. Ice algae biodiversity Nansen Legacy JC3 [Data set]. Norwegian Polar Institute, in the pipeline.

Assmy, P., Fernández-Méndez, M., Duarte, P., et al., 2017. Leads in Arctic pack ice enable early phytoplankton blooms below snow-covered sea ice. Sci. Rep. 7, 40850. https://doi.org/10.1038/srep40850.

Assmy, P., Kvernvik, A.C., Hop, H., et al., 2023. Seasonal plankton dynamics in Kongsfjorden during two years of contrasting environmental conditions. Prog. Oceanogr. 213, 102996 https://doi.org/10.1016/j.pocean.2023.102996.

Barber, D.G., Hop, H., Mundy, C.J., et al., 2015. Selected physical, biological and biogeochemical implications of a rapidly changing Arctic Marginal Ice Zone. Prog. Oceanogr. 139, 122–150. https://doi.org/10.1016/j.pocean.2015.09.003.

Barton, B.I., Lenn, Y.-D., Lique, C., 2018. Observed atlantification of the Barents Sea causes the Polar Front to limit the expansion of winter sea ice. Am. Meteorol. Soc. 48 (8), 1849–1866. https://doi.org/10.1175/JPO-D-18-0003.1.

Bauch, H.A., Erlenkeuser, H., Bauch, D., Mueller-Lupp, T., Taldenkova, E., 2004. Stable oxygen and carbon isotopes in modern benthic foraminifera from the Laptev Sea shelf: implications for reconstructing proglacial and profluvial environments in the Arctic. Mar. Micropaleontol. 51 (3–4), 285–300. https://doi.org/10.1016/j.marmicro.2004.01.002.

Berge, J., Renaud, P.E., Darnis, G., Cottier, C., Last, K., Gabrielsen, T.M., Johnsen, G., Seuthe, L., Weslawski, J.M., Leu, E., Moline, M., Nahrgang, J., Søreide, J.E., Varpe, Ø., Lønne, O.J., Daase, M., Falk-Petersen, S., 2015. In the dark: a review of ecosystem processes during the Arctic polar night. Prog. Oceanogr. 139, 258–271. https://doi.org/10.1016/j.pocean.2015.08.005.

Berge, J., Johnsen, G., Cohen, J.H., 2020. Polar night Marine Ecology. In: Life and Light in the Dead of Night. Advances in Polar Ecology. Springer Chem, p. 375. https://doi.org/10.1007/978-3-030-33208-2.

Bertlich, J., Gussone, N., Berndt, J., et al., 2021. Salinity effects on cultured Neogloboquadrina pachyderma (sinistral) from high latitudes: new paleoenvironmental insights. Geo-Mar. Lett. 41, 2. https://doi.org/10.1007/s00367-020-00677-1.

Bluhm, B.A., Swadling, K.M, Gradinger, R., 2017. Sea ice as a habitat for macrograzers. In: Thomas, D.N. (Eds.), Sea ice, third edition, Wiley Online Library. doi: 10.1002/9781118778371.ch16.

Bluhm, B.A., Hop, H., Vihtakari, M., et al., 2018. Sea ice meiofauna distribution on local to pan-Arctic scales. Ecol. Evol. 8 (4), 2350–2364. https://doi.org/10.1002/ece3.3797.

Bodur, Y.V., Renaud, P.E., Goraguer, L., et al., 2023. Seasonal patterns of vertical flux in the northern Barents Sea under Atlantic Water influence and sea-ice decline. Under revision for Progress of Oceanography. https://doi.org/10.1016/j.pocean.2023.103132.

Boetius, A., Albrecht, S., Bakker, K., et al., 2013. Export of algal biomass from the melting Arctic sea ice. Science 339 (6126), 1430–1432. https://doi.org/10.1126/science.1231346.

C3S, 2023. Sea ice edge and type v3.0 daily gridded data from 1978 to present derived from satellite observations. Copernicus Climate Change Service (C3S), Climate Data Store (CDS). doi: 10.24381/cds.29c46d83 [Accessed 2023 May].

Carey Jr, A.G., 1985. Marine ice fauna: Arctic. In: Horner, R.A. (Ed.), Sea ice biota. CRC Press, Boca Raton, pp. 173–190.

Carey Jr, A.G., 1992. The ice fauna in the shallow southwestern Beaufort Sea, Arctic Ocean. J. Mar. Syst. 3 (3), 225–236. https://doi.org/10.1016/0924-7963(92)90002-P.

Carey Jr, A.G., Montagna, P.A., 1982. Arctic sea ice faunal assemblage: first approach to description and source of the underice meiofauna. Mar. Ecol. Prog. Ser. 8 (1), 1–8. https://doi.org/10.3354/meps008001.

Cautain, I.J., Last, K.S., McKee, D., Bluhm, B.A., Renaud, P.E., Ziegler, A.F., Narayanaswamy, B.E., 2022. Uptake of sympagic organic carbon by the Barents Sea benthos linked to sea ice seasonality. Front. Mar. Sci. 9, 1009303. https://doi.org/10.3389/fmars.2022.1009303.

Chevenet, F., Doléadec, S., Chessel, D., 1994. A fuzzy coding approach for the analysis of long-term ecological data. Freshw. Biol. 31, 295–309. https://doi.org/10.1111/j.1365-2427.1994tb01742.x.

Cohen, J., Zhang, X., Francis, J., et al., 2020. Divergent consensuses on Arctic amplification influence on midlatitude severe winter weather. Nat. Clim. Chang. 10, 20–29. https://doi.org/10.1038/s41558-019-0662-y.

Comiso, J.C., Parkinson, C.L., Gersten, R., Stock, L., 2008. Accelerated decline in the Arctic sea ice cover. Geophys. Res. Lett. 35 (1) https://doi.org/10.1029/2007GL031972.

Conover, R.J., Harris, L.R., Bedo, A.W., 1991. Copepods in cold oligotrophic waters – How do they cope? Proceedings of the Fourth International Conference on Copepoda, Bulletin of the Plankton Society of Japan Special Volume, pp. 177–199.

Cox, G.F.N., Weeks, W.F., 1983. Equations for determining the gas and brine volumes in sea-ice samples. J. Glaciol. 29 (102), 306–316. https://doi.org/10.3189/S0022143000008364.

de Freitas, T.R., Bacalhau, E.T., Disaró, S.T., 2021. Biovolume method for foraminiferal biomass assessment: Evaluation of geometric models and incorporation of species mean cell occupancy. J. Foramin. Res. 51 (4), 249–266. https://doi.org/10.2113/gsjfr.51.4.249.

Degen, R., Aune, M., Bluhm, B.A., Cassidy, C., Kedra, M., Kraan, C., Vandepitte, L., Wlodarska-Kowalczuk, M., Zhulay, I., Albano, P.G., Bremner, J., Grebmeier, J.M., Link, H., Morata, N., Nordström, M.C., Shojaei, M.G., Sutton, L., Zuschin, M., 2018. Trait-based approaches in rapidly changing ecosystems: a roadmap to the future polar oceans. Ecol. Ind. 91, 722–736. https://doi.org/10.1016/j.ecolind.2018.04.050.

Dieckmann, G.S., Spindler, M., Lange, M.A., Ackley, S.F., Eicken, H., 1991. Antarctic sea ice: A habitat for the foraminifer *Neogloboquadrina pachyderma*. J. Foramin. Res. 21, 182–189.

Dörr, J., Årthun, M., Eldevik, T., Madonna, E., 2021. Mechanisms of regional winter sea-ice variability in a warming Arctic. J. Clim. 34 (21), 8635–8653. https://doi.org/10.1175/JCLI-D-21-0149.1.

Duarte, P., Sundfjord, A., Meyer, A., Hudson, S.R., Spreen, G., Smedsrud, L.H., 2020. WarmAtlantic water explains observed sea ice melt rates north of Svalbard. J. Geophys. Res. Oceans 125, e2019JC015662. https://doi.org/10.1029/2019JC015662.

Edler, L., Elbraechter, M., 2010. The Utermoehl method for quantitative phytoplankton analysis. In: Karlson, B. (Ed.), Microscopic and Molecular Methods for Quantitative Phytoplankton Analysis. United Nations Educational, Scientific and Cultural Organization (UNESCO), Paris, pp. 13–20.

Efstahiou, E., Eldevik, T., Årthun, M., Lind, S., 2022. Spatial patterns, pechanisms, and predictability of Barents sea ice change. J. Clim. 35 (10), 2961–2973. https://doi.org/10.1175/JCLI-D-21-0044.1.

Ehrlich, J., Schaafsma, F.L., Bluhm, B.B., Peeken, I., Castellani, G., Brandt, A., Flores, H., 2020. Sympagic fauna in and under Arctic pack ice in the annual sea-ice system of the new Arctic. Front. Mar. Sci. 7, 452. https://doi.org/10.3389/fmars.2020.00452.

Ehrlich, J., Bluhm, B.B., Peeken, I., Massicotte, P., Schaafsma, F.L., Castellani, G., Brandt, A., Flores, H., 2021. Sea-ice associated carbon flux in Arctic spring. Elem. Sci. Anth. 9, 1. https://doi.org/10.1525/elementa.2020.00169.

Fadeev, E., Rogge, A., Ramondenc, S., Nöthig, E.M., Wekerle, C., Bienhold, C., Salter, I., Waite, A.M., Hehemann, L., Boetius, A., Iversen, M.H., 2021. Sea ice presence is linked to higher carbon export and vertical microbial connectivity in the Eurasian Arctic Ocean. Commun. Biol. 4 (1), 1255. https://doi.org/10.1038/s42003-021-02776-w.

Feng, Z., Rubao, J., Ashjian, C., Zhand, J., Campbell, R., Grebmeier, J.M., 2021. Benthic hotspots on the northern Bering and Chukchi continental shelf: Spatial variability in production regimes and environmental drivers. Prog. Oceanogr. 191, 102497 https://doi.org/10.1016/j.pocean.2020.102497.

Fernández-Méndez, M., Wenzhöfer, F., Peeken, I., Sørensen, H.L., Glud, R.N., Boetius, A., 2014. Composition, buoyancy regulation and fate of ice algal aggregates in the Central Arctic Ocean. PLoS One 9, e107452.

Fernández-Méndez, M., Katlein, C., Rabe, B., Nicolaus, M., Peeken, I., Bakker, K., et al., 2015. Photosynthetic production in the central Arctic Ocean during the record sea-ice minimum in 2012. Biogeosciences 12, 3525–3549. https://doi.org/10.5194/bg-12-3525-2015.

Fernández-Méndez, M., Olsen, L.M., Kauko, H.M., et al., 2018. Algal Hot Spots in a Changing Arctic Ocean: Sea-Ice Ridges and the Snow-Ice Interface. Front. Mar. Sci. 5, 75. https://doi.org/10.3389/fmars.2018.00075.

Fossile, E., Nardelli, M.P., Jouini, A., Lansard, B., Pusceddu, A., Moccia, D., Michel, E., Péron, O., Howa, H., Mojtahid, M., 2020. Benthic foraminifera as tracers of brine production in the Storfjorden "sea ice factory". Biogeosciences 17, 1933–1953. https://doi.org/10.5194/bg-17-1933-2020.

Friedrich, C., 1997. Ökologische Untersuchungen zur Fauna des arktischen Meereises. Doctoral thesis, Berichte zur Polarforschung 246. Alfred-Wegener-Institut für Polar- und Meeresforschung, Bremerhaven, p. 211.

Friedrich, C., De Smet, W.H., 2000. The rotifer fauna of Arctic sea ice from the Barents Sea, Laptev Sea and Greenland Sea. Hydrobiologia 432, 73–89.

Golden, K.M., Ackley, S.F., Lytle, V.I., 1998. The percolation phase transition in sea ice. Science 282, 2238–2241. https://doi.org/10.1126/science.282.5397.2238.

Golden, K.M., Eicken, H., Heaton, A.L., Miner, J., Pringle, D.J., Zhu, J., 2007. Thermal evolution of permeability and microstructure in sea ice. Geophys. Res. Lett. 34, L16501. https://doi.org/10.1029/2007GL030447.

Goldstein, S.T., 1999. Foraminifera: A biological overview. In: Sen Gupta, B.K. (Ed.), Modern Foraminifera, Springer Dordrecht, 2022, pp. 37–55. doi: 10.1007/0-306-48104-9.

Gosselin, M., Legendre, L., Therriault, J.-C., Demers, S., 1990. Light and nutrient limitation of sea-ice microalgae (Hudson Bay, Canadian Arctic). J. Phycol. 26, 220–232. https://doi.org/10.1111/j.0022-3646.1990.00220.x.

Gosselin, M., Levasseur, M., Wheeler, P.A., Horner, R.A., Booth, B.C., 1997. New measurements of phytoplankton and ice algal production in the Arctic Ocean. Deep Sea Res. II 44, 1623–1644. https://doi.org/10.1016/S0967-0645(97)00054-4.

Gradinger, R., 1999. Vertical fine structure of algal biomass and composition in Arctic pack ice. Mar. Biol. 133, 745–754. https://doi.org/10.1007/s002270050516.

Gradinger, R., 2009. Sea-ice algae: Major contributors to primary production and algal biomass in the Chukchi and Beaufort Seas during May/June 2002. Deep Sea Res. Part II 56, 1201–1212. https://doi.org/10.1016/j.dsr2.2008.10.016.

Gradinger, R.R., Bluhm, B.A., Iken, K., 2010. Arctic sea-ice ridges-Safe havens for sea-ice fauna during periods of extreme ice melt? Deep-Sea Res. Part II: Top. Stud. Oceanogr. 57, 86–95. https://doi.org/10.1016/j.dsr2.2009.08.008.

Gradinger, R., Bluhm, B.A., 2020. First analysis of an Arctic sea ice meiofauna food web based on abundance, biomass and stable isotope ratios. Mar. Ecol. Prog. Ser. 634, 29–43. https://doi.org/10.3354/meps13170.

Gradinger, R., Ikävalko, J., 1998. Organism incorporation into newly forming Arctic sea ice in the Greenland Sea. J. Plankton Res. 2, 871–886. https://doi.org/10.1093/plankt/20.5.871.

Gradinger, R.R., Meiners, K., Plumley, G., Zhang, Q., Bluhm, B.A., 2005. Abundance and composition of the sea-ice meiofauna in off-shore pack ice of the Beaufort Gyre in summer 2002 and 2003. Polar Biol. 28, 171–181. https://doi.org/10.1007/s00300-004- 0674- 5.

Gradinger, R., Spindler, M., Henschel, D., 1991. Development of Arctic sea-ice organisms under graded snow cover. Polar Res. 10, 295–307. https://doi.org/10.3402/polar.v10i1.6748.

Gradinger, R., Friedrich, C., Spindler, M., 1999. Abundance, biomass and composition of the sea ice biota of the Greenland Sea pack ice. Deep-Sea Res. Part II-Top. Stud. Oceanogr. 46, 1457–1472. https://doi.org/10.1016/S0967-0645(99)00030-2.

Gradinger, R., Zhang, Q., 1997. Vertical distribution of bacteria in Arctic sea ice from the Barents and Laptev Seas. Polar Biol. 17, 448–454. https://doi.org/10.1007/s003000050139.

Grainger, E.H., Hsiao, S.I.C., Pinkewycz, N., Mohammed, A.A., Neuhof, V., 1985. The Food of Ice Fauna and Zooplankton in Frobisher Bay. Canadian Data Report of Fisheries and Aquatic Sciences 558, Arctic Biological Station, Quebéc, pp. 67.

Grainger, E.H., Hsiao, S.I.C., 1990. Trophic relationships of the sea ice meiofauna in Frobisher Bay, Arctic Canada. Polar Biol. 10, 283–292. https://doi.org/10.1007/BF00238427.

Granskog, M.A., Fer, I., Rinke, A., Steen, H., 2018. Atmosphere-Ice-Ocean- Ecosystem processes in a thinner arctic sea ice regime: the Norwegian young sea ICE (N-ICE2015) expedition. J. Geophys. Res. 123, 1586–1594. https://doi.org/10.1002/2017jc013328.

Grenvald, J.C., Callesen, T.A., Daase, M., et al., 2016. Plankton community composition and vertical migration during polar night in Kongsfjorden. Polar Biol. 39, 1879–1895. https://doi.org/10.1007/s00300-016-2015-x.

Gulliksen B., Lønne O.J., 1989. Distribution, abundance, and ecological importance of marine sympagic fauna in the Arctic. Rapports et procès-verbaux des réunions (1903–1991). Report, 188, 133-138. doi: 10.17895/ices.pub.19279244.v1.

Hancke, K., Lund-Hansen, L.C., Lamare, M.L., Højlund Pedersen, S., King, M.D., Andersen, P., Sorrell, B.K., 2018. Extreme low light requirement for algae growth underneath sea ice: a case study from station Nord, NE Greenland. J. Geophys. Res. Oceans 123, 985–1000. https://doi.org/10.1002/2017JC013263.

Hansen, A.S., Nielsen, T.G., Levinsen, H., Madsen, S.D., Thingstad, T.F., Hansen, B.W., 2003. Impact of changing ice cover on pelagic productivity and food web structure in Disko Bay, West Greenland: a dynamic model approach. Deep Sea Res. Part I 50 (1), 171–187. https://doi.org/10.1016/S0967-0637(02)00133-4.

Hardge, K., Peeken, I., Neuhaus, S., et al., 2017. The importance of sea ice for exchange of habitat-specific protist communities in the Central Arctic Ocean. J. Mar. Syst. 165, 124–138. https://doi.org/10.1016/j.jmarsys.2016.10.004.

Hegseth, E., 1998. Primary production of the northern Barents Sea. Polar Res. 17 (2), 113–123. https://doi.org/10.1111/j.1751-8369.1998.tb00266.x.

Hegseth, E.N., et al., 2019. Phytoplankton Seasonal Dynamics in Kongsfjorden, Svalbard and the Adjacent Shelf. In: Hop, H., Wiencke, C. (Eds.), The Ecosystem of Kongsfjorden, Svalbard. Advances in Polar Ecology, Vol. 2, Springer, Cham, pp. 173–229. https://doi.org/10.1007/978-3-319-46425-1.

Hegseth, E.N., von Quillfeldt, C., 2022. The Sub-Ice Algal Communities of the Barents Sea Pack Ice: Temporal and Spatial Distribution of Biomass and Species. J. Mar. Sci. Eng. 10, 164. https://doi.org/10.3390/jmse10020164.

Hillebrand, H., Dürselen, C.-D., Kirschtel, D., Pollingher, U., Zohary, T., 2002. Biovolume calculation for pelagic and benthic microalgae. J. Phycol. 35 (2), 403–424. https://doi.org/10.1046/j.1529-8817.1999.3520403.x.

Hirche, H.J., Kosobokova, K.N., 2011. Winter studies on zooplankton in Arctic seas: the Storfjord (Svalbard) and adjacent ice-covered Barents Sea. Mar. Biol. 158, 2359–2376. https://doi.org/10.1007/s00227-011-1740-5.

Hodal, H., Falk-Petersen, S., Hop, H., et al., 2012. Spring bloom dynamics in Kongsfjorden, Svalbard: nutrients, phytoplankton, protozoans and primary production. Polar Biol. 35, 191–203. https://doi.org/10.1007/s00300-011-1053-7.

Holm-Hansen, O., Riemann, B., 1978. Chlorophyll *a* determination: improvements in methodology. Oikos 30, 438–447. https://doi.org/10.2307/3543338.
Hop, H., Assmy, P., Wold, A., et al., 2019. Pelagic Ecosystem Characteristics Across the Atlantic Water Boundary Current From Rijpfjorden, Svalbard, to the Arctic Ocean During Summer (2010–2014). Front. Mar. Sci. 6, 181. https://doi.org/10.3389/fmars.2019.00181.
Hop, H., Vihtakari, M., Bluhm, B.A., Assmy, P., Poulin, M., Gradinger, R., Peeken, I., von Quillfeldt, C., Olsen, L.M., Zhitina, L., Melnikov, I.A., 2020. Changes in sea-ice protist diversity with declining sea ice in the Arctic Ocean from the 1980s to 2010s. Frontiers in Marine Science 7(243). doi: 10.3389/fmars.2020.00243.
Hop, H., Vihtakari, M., Bluhm, B.A., Daase, M., Gradinger, R., Melnikov, I.A., 2021. Ice-Associated Amphipods in a Pan-Arctic Scenario of Declining Sea Ice. Front. Mar. Sci. 8, 743152 https://doi.org/10.3389/fmars.2021.743152.
Horner, R., Schrader, G.C., 1982. Relative contributions of ice algae, phytoplankton, and benthic microalgae to primary production in nearshore regions of the Beaufort Sea. Arctic *35*(4), 485–503. http://www.jstor.org/stable/40509382.
Ingvaldsen, R.B., Assmann, K.M., Primicerio, R., et al., 2021. Physical manifestations and ecological implications of Arctic Atlantification. Nat. Rev. Earth Environ. 2, 874–889. https://doi.org/10.1038/s43017-021-00228-x.
Isaksen, K., Nordli, Ø., Ivanov, B., et al., 2022. Exceptional warming over the Barents area. Sci. Rep. 12, 9371. https://doi.org/10.1038/s41598-022-13568-5.
Jakobsson, M., 2002. Hypsometry and volume of the Arctic Ocean and its constituent seas. Geochem. Geophys. Geosyst. 3 (5) https://doi.org/10.1029/2001GC000302.
Johnsen, G., Hegseth, E.N., 1991. Photoadaptation of sea-ice microalgae in the Barents Sea. Polar Biol. 11, 179–184. https://doi.org/10.1007/BF00240206.
Johnsen, G., Leu, E., Gradinger, R., 2020. Marine Micro- and Macroalgae in the Polar Night. In: Berge, J., Jihnsen, G., Cohen, J.H. (Eds.), Polar Night Marine Ecology, Advances in Polar Ecology, Vol. 4. Springer, Cham, pp. 67–112. https://doi.org/10.1007/978-3-030-33208-2_4.
Jones, E., Fransson, A., Chierici, M., Divine, D., Ericson, Y., Hodal-Lødemel, H., Anglada-Ortiz G., Raffel, B., Zamelczyk, K., 2023. Sea ice salinity and temperature from cores collected in Barents Sea and Nansen Basin, 2018–2022 [Data set]. Norwegian Polar Institute. doi: 10.21334/npolar.2023.9622d925.
Kauko, H.M., Olsen, L.M., Duarte, P., Peeken, I., Granskog, M.A., Johnsen, G., Fernández-Méndez, M., Pavlov, A.K., Mundy, C.J., Assmy, P., 2018. Algal colonization of young Arctic sea ice in spring. Front. Mar. Sci. 5, 199. https://doi.org/10.3389/fmars.2018.00199.
Kern, J.C., Carey Jr, A.G., 1983. The faunal assemblage inhabiting seasonal sea ice in the nearshore Arctic Ocean with emphasis on copepods. Mar. Ecol. Prog. Ser. 10, 159–167.
Kiko, R., Kern, S., Kramer, M., Mütze, H., 2017. Colonization of newly forming Arctic sea ice by meiofauna: A case study for the future Arctic? Polar Biol. 40, 1277–1288. https://doi.org/10.1007/s00300-016-2052-5.
Kimura, N., Tateyama, K., Sato, K., Krishfield, R.A., Yamaguchi, H., 2020. Unusual drift behaviour of multi-year sea ice in the Beaufort Sea during summer 2018. Polar Res. 39 https://doi.org/10.33265/polar.v39.3617.
Kohlbach, D., Goraguer, L., Bodur, Y.V., Müller, O., Amargant-Arumí, M., Blix, K., Bratbak, G., Chierici, M., Dąbrowska, A.M., Dietrich, U., Edvardsen, B., García, L.M., Gradinger, G., Hop, H., Jones, J., Lundesgaard, Ø., Olsen, L.M., Reigstad, M., Saubrekka, K., Tatarek, A., Wiktor, J.M., Wold, A., Assmy, P., 2023. Earlier sea-ice melt extends the oligotrophic summer period in the Barents Sea with low algal biomass and associated low vertical flux. Prog. Oceanogr. 213, 103018 https://doi.org/10.1016/j.pocean.2023.103018.
Kosobokova, K.N., Hopcraft, R.R., Hirsche, H.-J., 2012. Patterns of zooplankton diversity through the depths of the Arctic's central basins. Mar. Biodivers. 41, 29–50. https://doi.org/10.1007/s12526-010-0057-9.
Kovacs, K.M., Lydersen, C., Overland, J.E., et al., 2011. Impacts of changing sea-ice conditions on Arctic marine mammals. Mar. Biodivers. 41, 181–194. https://doi.org/10.1007/s12526-010-0061-0.
Kramer, M., 2011. The role of sympagic meiofauna in Arctic and Antarctic sea-ice food webs. Christian-Albrecht University of Kiel. Dissertation.
Krembs, C., Eicken, H., Deming, J.W., 2011. Exopolymer alteration of physical properties of sea ice and implications for ice habitability and biogeochemistry in a warmer Arctic. Proc. Natl. Acad. Sci. 108 (9), 3653–3658. https://doi.org/10.1073/pnas.1100701108.
Krumpen, T., Belter, H.J., Boetius, A., Damm, E., Haas, C., Hendricks, S., Nicolaus, M., Nöthig, E.-M., Paul, S., Peeken, I., 2019. Arctic warming interrupts the Transpolar Drift and affects long-range transport of sea ice and ice-rafted matter. Sci. Rep. 9 (1), 5459. https://doi.org/10.1038/s41598-019-41456-y.
Kuhn, M., Jackson, S., Cimentada, J., 2022. corrr: Correlations in R. R package version 0.4.4. https://CRAN.R-project.org/package=corrr.
Kwok, R., 2009. Outflow of Arctic Ocean sea ice into the Greenland and Barents Seas: 1979–2007. J. Clim. 22, 2438–2457. https://doi.org/10.1175/2008JCLI2819.1.
Kwok, R., 2018. Arctic sea ice thickness, volume, and multiyear ice coverage: losses and coupled variability (1958–2018). Environ. Res. Lett. 13, 105005 https://doi.org/10.1088/1748-9326/aae3ec.
Leppäranta, M., Manninen, T., 1988. The brine and gas content of sea ice with attention to low salinities and high temperatures. Finnish Institute of Marine Research Internal Report 88, pp. 1–148.
Leu, E., Søreide, J.E., Hessen, D.O., Falk-Petersen, S., Berge, J., 2011. Consequences of changing sea-ice cover for primary and secondary producers in the European Arctic shelf seas: Timing, quantity, and quality. Prog. Oceanogr. 90 (1–4), 18–32. https://doi.org/10.1016/j.pocean.2011.02.004.
Leu, E., Mundy, C.J., Assmy, P., Campbell, K., Gabrielsen, T.M., Gosselin, M., Juul-Pedersen, T., Gradinger, R., et al., 2015. Arctic spring awakening – Steering principles behind the phenology of vernal ice algal blooms. Prog. Oceanogr. 139, 151–170. https://doi.org/10.1016/j.pocean.2015.07.012.
Lind, S., Ingvaldsen, R.B., 2012. Variability and impacts of Atlantic Water entering the Barents Sea from the north. Deep-Sea Res. 62, 70–88. https://doi.org/10.1016/j.dsr.2011.12.007.
Lind, S., Ingvaldsen, R.B., Furevik, T., 2018. Arctic warming hotspot in the northern Barents Sea linked to declining sea-ice import. Nat. Clim. Chang. 8, 634–639. https://doi.org/10.1038/s41558-018-0205-y.
Loeng, H., 1991. Features of the physical oceanographic conditions of the Barents Sea. Polar Res. 10 (1), 5–18. https://doi.org/10.1111/j.1751-8369.1991.tb00630.x.
Lukina, T.G., 2001. Foraminifera of the Laptev Sea. Protistology 2 (2), 105–122.
Lundesgaard, Ø., Sundfjord, A., Lind, S., Nilsen, F., Renner, A.H.H., 2022. Import of Atlantic Water and sea ice controls the ocean environment in the northern Barents Sea. Ocean Sci. 18 (5), 1389–1418. https://doi.org/10.5194/os-18-1389-2022.
Lund-Hansen, L.C., Søgaard, D.H., Sorrell, B.K., Gradinger, R., Meiners, K.M., 2020. Arctic Sea Ice Ecology. Seasonal Dynamics in Algal and Bacterial Productivity. Springer Cham, pp. 178. doi: 10.1007/978-3-030-37472-3.
Lund-Hansen, L.C., Hawes, I., Nielsen, M.H., Sorrell, B.K., 2017. Is colonization of sea ice by diatoms facilitated by increased surface roughness in growing ice crystals? Polar Biol. 40, 593–602. https://doi.org/10.1007/s00300-016-1981-3.
Marquardt, M., Kramer, M., Carnat, G., Werner, I., 2011. Vertical distribution of sympagic meiofauna in sea ice in the Canadian Beaufort Sea. Polar Biol. 34, 1887–1900. https://doi.org/10.1007/s00300-011-1078-y.
Marquardt, M., Majaneva, S., Pitusi, V., Søreide, J.E., 2018. Pan-Arctic distribution of the hydrozoan Sympagohydra tuuli? First record in sea ice from Svalbard (European Arctic). Polar Biol. 41, 583–588. https://doi.org/10.1007/s00300-017-2219-8.
Marquardt, M., Bodur, Y.V., Dubourg, P., Reigstad, M., 2022a. Concentration of Particulate Organic Carbon (POC) and Particulate Organic Nitrogen (PON) from the sea water and sea ice in the northern Barents Sea as part of the Nansen Legacy project, Cruise 2019706 Q3 [Data set]. Norstore. https://doi.org/10.11582/2022.00055.
Marquardt, M., Bodur, Y.V., Dubourg, P., Reigstad, M., 2022b. Concentration of Particulate Organic Carbon (POC) and Particulate Organic Nitrogen (PON) from the sea water and sea ice in the northern Barents Sea as part of the Nansen Legacy project, Cruise 2019711 Q4 [Data set]. Norstore. https://doi.org/10.11582/2022.00048.
Marquardt, M., Bodur, Y.V., Dubourg, P., Reigstad, M., 2022c. Concentration of Particulate Organic Carbon (POC) and Particulate Organic Nitrogen (PON) from the sea water and sea ice in the northern Barents Sea as part of the Nansen Legacy project, Cruise 2021703 Q1 [Data set]. Norstore. https://doi.org/10.11582/2022.00053.
Marquardt, M., Bodur, Y.V., Dubourg, P., Reigstad, M., 2022d. Concentration of Particulate Organic Carbon (POC) and Particulate Organic Nitrogen (PON) from the sea water and sea ice in the northern Barents Sea as part of the Nansen Legacy project, Cruise 2021704 Q2 [Data set]. Norstore. https://doi.org/10.11582/2022.00054.
Marquardt, M., Goraguer, L., Duborg, P., Reigstad, M., 2022e. Concentration of Particulate Organic Carbon (POC) and Particulate Organic Nitrogen (PON) from the sea water and sea ice in the northern Barents Sea as part of the Nansen Legacy project, Cruise 2021708 JC2-1 [Data set]. Norstore. https://doi.org/10.11582/2022.00050.
Marquardt, M., Patrohay, E., Goraguer, L., Dubourg, P., Reigstad, M., 2022f. Concentration of Particulate Organic Carbon (POC) and Particulate Organic Nitrogen (PON) from the sea water and sea ice in the northern Barents Sea as part of the Nansen Legacy project, Cruise 2022702 JC3 [Data set]. Norstore.
Marquardt, M., Bluhm, B., Gradinger, R., 2023a. Sea-ice meiofauna biodiversity from the Nansen Legacy cruise Q3 (cruise number: 2019706) [Data set]. Norstore. https://doi.org/10.11582/2023.00084.
Marquardt, M., Bluhm, B., Gradinger, R., 2023b. Sea-ice meiofauna biodiversity from the Nansen Legacy cruise Q4 (cruise number: 2019711) [Data set]. Norstore. https://doi.org/10.11582/2023.00078.
Marquardt, M., Bluhm, B., Gradinger, R., 2023c. Sea-ice meiofauna biodiversity from the Nansen Legacy cruise Q2 (cruise number: 2021704) [Data set]. Norstore. https://doi.org/10.11582/2023.00082.
Marquardt, M., Pitusi, V., Bluhm, B., Gradinger, R., 2023d. Sea-ice meiofauna biodiversity from the Nansen Legacy cruise JC2-1 (cruise number: 2021708) [Data set]. Norstore. https://doi.org/10.11582/2023.00077.
Marquardt, M., Patrohay, E., Goraguer, L., Bluhm, B., Gradinger, R., 2023e. Sea-ice meiofauna biodiversity from the Nansen Legacy cruise JC3 (cruise number: 2022702) [Data set]. Norstore. https://doi.org/10.11582/2023.00081.
Marquardt, M., Hop, H., Keck Al-Habahbeh, A., Leopold, P., Vihtakari, M., Bluhm, B., Gradinger, R., 2023f. Sea-ice associated fauna biodiversity sampled by divers under the ice from the Nansen Legacy cruise Q2 (cruise number: 2021704) [Data set]. Norstore. https://doi.org/10.11582/2023.00083.
Marshall Jr., J.T., 1949. The endemic avifauna of Saipan, Tinian, Guam, and Palau. Condor 51, 200–222.
Melle, W., Skjoldal, H.-R., 1989. Zooplankton reproduction in the Barents Sea vertical distribution of eggs and nauplii of *Calanus finmarchicus* in relation to spring phytoplankton development. In: Ryland, J.S., Tyler, P.A. (Eds.), Reproduction. Genetics and Distribution of Marine Organisms, Olsen and Olsen, Fredensborg, Denmark, pp. 137–146.
Melnikov, I.A., 1989. Ecosystem of the Arctic sea ice. PP Shirshov Inst Oceanol Moscow, Akad Nauk SSSR, p. 191 (in Russian).
Melnikov, I.A., 1997. The Arctic Sea ice ecosystem. Gordon and Breach Science Publishers, Amsterdam, p. 204.

Menden-Deuer, S., Lessard, E.J., 2000. Carbon to volume relationships for dinoflagellates, diatoms, and other protist plankton. Limnol. Oceanogr. 45 (3), 569–579. https://doi.org/10.4319/lo.2000.45.3.0569.
Michel, C., Nielsen, T.G., Nozais, C., Gosselin, M., 2002. Significance of sedimentation and grazing by ice micro- and meiofauna for carbon cycling in annual sea ice (northern Baffin Bay). Aquat. Microb. Ecol. 30, 57–68. https://doi.org/10.3354/ame030057.
Mock, T., Gradinger, R., 1999. Determination of Arctic ice algal production with a new and easy *in situ* incubation technique. Mar. Ecol. Prog. Ser. 177, 15–26.
Møller, E.F., Nielsen, T.G., 2020. Borealization of Arctic zooplankton—smaller and less fat zooplankton species in Disko Bay. Western Greenland Limnol. Oceanogr. 65 (6), 1175–1188. https://doi.org/10.1002/lno.11380.
Montresor, M., Lovejoy, C., Orsini, L., Procacci, G., Roy, S., 2003. Bipolar distribution of the cyst-forming dinoflagellate Polarella glacialis. Polar Biol. 26, 186. https://doi.org/10.1007/s00300-002-0473-9.
Moon, T.A., Thoman, R., Druckenmiller, M.L., (Eds.), 2023. The Arctic. In: State of the Climate in 2022, Bulletin of the American Meteorological Society, 104 (9), S271–S321. doi: 10.1175/10.1175/BAMS-D-23-0079.1.
Mundy, C.J., Barber, D.G., Michel, C., 2005. Variability of snow and ice thermal, physical and optical properties pertinent to sea ice algae biomass during spring. J. Mar. Syst. 58 (3–4), 107–120. https://doi.org/10.1016/j.jmarsys.2005.07.003.
Mundy, C.J., Ehn, J.K., Barber, D.G., Michel, C., 2007. Influence of snow cover and algae on the spectral dependence of transmitted irradiance through Arctic landfast first-year sea ice. J. Geophys. Res. Oceans 112 (C3). https://doi.org/10.1029/2006JC003683.
Niemi, A., Michel, C., Hille, K., Poulin, M., 2011. Protist assemblages in winter sea ice: setting the stage for the spring ice algal bloom. Polar Biol. 34, 1803–1817. https://doi.org/10.1007/s00300-011-1059-1.
Nozais, C., Gosselin, M., Michel, C., Tita, G., 2001. Abundance, biomass, composition and grazing impact of the sea-ice meiofauna in the North Water, northern Baffin Bay. Mar. Ecol. Prog. Ser. 217, 235–250. https://doi.org/10.3354/meps217235.
Oksanen, J., Simpson, G., Blanchet, F., et al., 2022. vegan: Community Ecology Package. R package version 2.6-4, https://CRAN.R-project.org/package=vegan.
Olsen, L.M., Laney, S.R., Duarte, P., et al., 2017. The seeding of ice algal blooms in Arctic pack ice: The multiyear ice seed repository hypothesis. J. Geophys. Res. Biogeo. 122, 1529–1548. https://doi.org/10.1002/2016JG003668.
Onarheim, I.H., Årthun, M., 2017. Toward an ice-free Barents Sea. Geophys. Res. Lett. 44 (16), 8387–8395. https://doi.org/10.1002/2017GL074304.
OSI SAF, 2010. Global Low Resolution Sea Ice Drift - Multimission, EUMETSAT SAF on Ocean and Sea Ice. doi: 10.15770/EUM_SAF_OSI_NRT_2007.
OSI SAF, 2022a. Global Sea Ice Drift Climate Data Record Release v1.0 - Multimission, EUMETSAT SAF on Ocean and Sea Ice. doi: 10.15770/EUM_SAF_OSI_0012.
OSI SAF, 2022b. Global Sea Ice Concentration Climate Data Record v3.0 - Multimission, EUMETSAT SAF on Ocean and Sea Ice. doi: 10.15770/EUM_SAF_OSI_0013.
OSI SAF, 2022c. Global Sea Ice Concentration Interim Climate Data Record Release 3 - DMSP, EUMETSAT SAF on Ocean and Sea Ice. doi: 10.15770/EUM_SAF_OSI_0014.
OSI SAF, 2023. EUMETSAT Ocean and Sea Ice Satellite Application Facility, Sea ice index 1978-onwards (v2.2, 2023), OSI-420, available from https://osisaf-hl.met.no/v2p2-sea-ice-index.
Pagano, A.M., Williams, T.M., 2021. Physiological consequences of Arctic sea ice loss on large marine carnivores: unique responses by polar bears and narwhals. J. Exp. Biol. 224, jeb228049. https://doi.org/10.1242/jeb.228049.
Passow, U., 1991. Species-specific sedimentation and sinking velocities of diatoms. Mar. Biol. 108, 449–455. https://doi.org/10.1007/BF01313655.
Patrohay, E., Gradinger, R., Marquardt, M., Bluhm, B.A., 2022. First trait-based characterization of Arctic ice meiofauna taxa. Polar Biol. 45, 1673–1688. https://doi.org/10.1007/s00300-022-03099-0.
Petrich, C., Eicken, H., 2016. Overview of sea ice growth and properties. In: Thomas, D. N. (Ed.), Sea Ice, Third Edition, Wiley Online Library. doi: 10.1002/9781118778371.ch1.
Poulin, M., Cardinal, A., 1982. Sea ice diatoms from Manitounuk Sound, southeastern Hudson Bay (Quebec, Canada). II. Naviculaceae, genus *Navicula*. Can. J. Bot. 60(12), 2825–2845.
Poulin, M., Daugbjerg, N., Gradinger, R., et al., 2011. The pan-Arctic biodiversity of marine pelagic and sea-ice unicellular eukaryotes: a first-attempt assessment. Mar. Biodivers. 41, 13–28. https://doi.org/10.1007/s12526-010-0058-8.
Ratkova, T.N., Wassmann, P., 2005. Sea ice algae in the White and Barents seas: composition and origin. Polar Res. 24, 95–110. https://doi.org/10.3402/polar.v24i1.6256.
Redfield, A.C., Ketchum, B.H., Richards, F.A., 1963. The influence of organisms on the composition of sea-water. In: Hill, M.N. (Ed.), The composition of seawater: Comparative and descriptive oceanography. Interscience Publishers, New York, pp. 26–77.
Reigstad, M., Riser, C.W., Wassmann, P., Ratkova, T., 2008. Vertical export of particulate organic carbon: Attenuation, composition and loss rates in the northern Barents Sea. Deep-Sea Res. II 55, 2308–2319. https://doi.org/10.1016/j.dsr2.2008. 05.007.
Revelle, W., 2023. psych: Procedures for Psychological, Psychometric, and Personality Research. Northwestern University, Evanston, Illinois. Rpackage version 2.3.3, https://CRAN.R-project.org/package=psych.
Riebesell, U., Schloss, I., Smetacek, V., 1991. Aggregation of algae released from melting sea ice: implications for seeding and sedimentation. Polar Biol. 11, 239–248. https://doi.org/10.1007/BF00238457.
Sakshaug, E., Johnsen, G., Kristiansen, S., von Quilfeldt, C.H., Rey, F., Slagstad, D., Thingstad, F., 2009. Phytoplankton and primary productions. In: Sakshaug, E., Johnsen, G., Kovacs, K.M. (Eds.), Ecosystem Barents Sea. Tapir Academic Press, Trondheim, pp. 167–208.
Schiebel, R., Hemleben, C., 2017. Planktic Foraminifers in the Modern Ocean. Second Edition. Springer-Verlag, Berlin Heidelberg. doi: 10.1007/978-3-662-50297-6.
Schünemann, H., Werner, I., 2005. Seasonal variations in distribution patterns of sympagic meiofauna in Arctic pack ice. Mar. Biol. 146, 1091–1102. https://doi.org/10.1007/s00227-004-1511-7.
Screen, J., Simmonds, I., 2010. The central role of diminishing sea ice in recent Arctic temperature amplification. Nature 464, 1334–1337. https://doi.org/10.1038/nature09051.
Seidenkrantz, M.-S., 2013. Benthic foraminifera as palaeo sea-ice indicators in the subarctic realm – examples from the Labrador Sea-Baffin Bay region. Quat. Sci. Rev. 79, 135–144. https://doi.org/10.1016/j.quascirev.2013.03.014.
Sherr, E.B., Sherr, B.F., Wheeler, P.A., Thompson, K., 2003. Temporal and spatial variation in stocks of autotrophic and heterotrophic microbes in the upper water column of the central Arctic Ocean. Deep Sea Res., Part I 50, 557–571. https://doi.org/10.1016/S0967-0637(03)00031-1.
Siwertsson, A., Husson, B., Arneberg, P., et al., 2023. Panel-based Assessment of Ecosystem Condition of Norwegian Barents Sea shelf ecosystems. Report, Rapport fra havforskningen Nr. 2023-14. https://www.hi.no/hi/nettrapporter/rapport-fra-havforskningen-en-2023-14.
Smedsrud, L.H., Ingvaldsen, R., Nilsen, J.E.Ø., Skagseth, Ø., 2010. Heat in the Barents Sea: transport, storage, and surface fluxes. Ocean Sci. 6 (1), 219–234. https://doi.org/10.5194/os-6-219-2010.
Smetacek, V., Nicol, S., 2005. Polar ocean ecosystems in a changing world. Nature 437 (7057), 362–368. https://doi.org/10.1038/nature04161.
Søreide, J.E., Leu, E., Berge, J., Graeve, M., Falk-Petersen, S., 2010. Timing of blooms, algal food quality and *Calanus glacialis* reproduction and growth in a changing Arctic. Glob. Chang. Biol. 16 (11), 3154–3163. https://doi.org/10.1111/j.1365-2486.2010.02175.x.
Spindler, M., 1994. Notes on the biology of sea ice in the Arctic and Antarctic. Polar Biol. 14, 319–324. https://doi.org/10.1007/BF00238447.
Steer, A., Divine, D., 2023. Sea ice concentrations in the northern Barents Sea and the area north of Svalbard at Nansen Legacy stations during 2017-2021 [Data set]. Norwegian Polar Institute. doi: 10.21334/npolar.2023.24f2939c.
Stige, L.C., Rogers, L.A., Neuheimer, A.B., et al., 2019. Density- and size-dependent mortality in fish early life stages. Fish Fish. 20 (5), 962–976. https://doi.org/10.1111/faf.12391.
Stoecker, D.K., Gustafson, D.E., Black, M.M.D., Baier, C.T., 1998. Population dynamics of microalgae in the upper land-fast sea ice at a snow-free location. J. Phycol. 34 (1), 60–69. https://doi.org/10.1046/j.1529-8817.1998.340060.x.
Stroeve, J., Notz, D., 2018. Changing state of Arctic sea ice across all seasons. Environ. Res. Lett. 13, 103001 https://doi.org/10.1088/1748-9326/aade56.
Syvertsen, E.E., 1991. Ice algae in the Barents Sea: types of assemblages, origin, fate and role in the ice-edge phytoplankton bloom. Polar Res. 10 (1) https://doi.org/10.1111/j.1751-8369.1991.tb00653.x.
Tamelander, T., Kivimäe, C., Bellerby, R.G.J., Renaud, P.E., Kristiansen, S., 2009. Baseline variations in stable isotope values in an Arctic marine ecosystem: effects of carbon and nitrogen uptake by phytoplankton. Hydrobiologia 630, 63–73. https://doi.org/10.1007/s10750-009-9780-2.
Tedesco, L., Vichi, M., Scoccimarro, E., 2019. Sea-ice algal phenology in a warmer Arctic. Sci. Adv. 5, eaav4830 https://doi.org/10.1126/sciadv.aav4830.
The Nansen Legacy, 2022. Sampling Protocols: Version 10. The Nansen Legacy Report Series 32/2022. doi: 10.7557/nlrs.6684.
Timchenko, A.I., Syomin, V.L., Portnova, D.A., 2021. Sympagic fauna in the northern part of the Barents Sea and adjacent Nansen Basin. Reg. Stud. Mar. Sci. 47, 101920 https://doi.org/10.1016/j.rsma.2021.101930.
Torstensson, A., Showalter, G.M., Margolin, A.R., Shadwick, E.H., Deming, J.W., Smith Jr., W.O., 2023. Chemical and biological vertical distributions withing central Arctic (>82 N) sea ice during late summer. Mar. Ecol. Prog. Ser. 703, 17–30. doi: 10.3354/meps14213.
Tschudi, M., Meier, W.N., Stewart, J.S., Fowler, C., Maslanik, J. 2019. EASE-Grid Sea Ice Age, Version 4. Boulder, Colorado, USA. NASA National Snow and Ice Data center Distributed Active Snow and Ice Data Center. doi: 10.5067/UTAV7490FEPB.[Date: June 2023].
Uye, S., Aoto, I., Onbé, T., 2002. Seasonal population dynamics and production of *Microsetella norvegica*, a widely distributed but little-studied marine planktonic harpacticoid copepod. J. Plankton Res. 24 (2), 143–153. https://doi.org/10.1093/plankt/24.2.143.
Vader, A., et al., unpublished. Chlorophyll A and phaeopigments Nansen Legacy cruise 2022702 [Data set], in the pipeline.
Vader, A., Marquardt, M., Bodur, Y., 2022a. Chlorophyll A and phaeopigments Nansen Legacy cruise 2019706. [Data set]. Norwegian Marine Data Centre. doi: 10.21335/NMDC-1109067467.
Vader, A., Marquardt, M., Amundsen, R., Bodur, Y., 2022b. Chlorophyll A and phaeopigments Nansen Legacy cruise 2019711. [Data set]. Norwegian Marine Data Centre. doi: 10.21335/NMDC-226850212.
Vader, A., Marquardt, M., Chitkara, C., Bodur, Y., 2022c. Chlorophyll A and phaeopigments Nansen Legacy cruise 2021703. [Data set]. Norwegian Marine Data Centre. doi: 10.21335/NMDC-983908955.
Vader, A., Marquardt, M., Summers, N., Flo, S., Assmy, P., 2022d. Chlorophyll A and phaeopigments Nansen Legacy cruise 2021704. [Data set]. Norwegian Marine Data Centre. doi: 10.21335/NMDC-966499899.
Vader, A., Goraguer, L., Marsden, L., 2022e. Chlorophyll A and phaeopigments Nansen Legacy cruise 2021708. [Data set]. Norwegian Marine Data Centre. doi: 10.21335/NMDC-1248407516.

Vader, A., Marquardt, M., Meshram, A.R., Gabrielsen, T.M., 2015. Key Arctic phototrophs are widespread in the polar night. Polar Biol. 38, 13–21. https://doi.org/10.1007/s00300-014-1570-2.

Volkmann, R., 2000. Planktic Foraminifers in the Outer Laptev Sea and the Fram Strait–Modern Distribution and Ecology. J. Foraminiferal Res. 30, 157–176. doi: 10.2113/0300157.

von Quillfeldt, C.H., 2000. Common diatom species in arctic spring blooms: their distribution and abundance. Bot. Mar. 43, 499–516. https://doi.org/10.1515/BOT.2000.050.

von Quillfeldt, C.H., Ambrose, W.G., Clough, L.M., 2003. High number of diatom species in first year ice from the Chukchi Sea. Polar Biol. 26, 806–818. https://doi.org/10.1007/s00300-003-0549-1.

Wassmann, P., 2022. The Nansen Legacy: pioneering research beyond the present ice edge of the Arctic Ocean. In: Auad, G., Wiese, F.K. (Eds.), Partnerships in Marine Research: Case Studies, Lessons Learned, and Policy Implications. Elsevier, pp. 33–51.

Wassmann, P., Duarte, C.M., Agustí, S., Sejr, M.K., 2011. Footprints of climate change in the Arctic marine ecosystem. Glob. Chang. Biol. 12, 1235–1249. https://doi.org/10.1111/j.1365-2486.2010.02311.x.

Wei, T., Simko, V., 2021. R package 'corrplot': Visualization of a Correlation Matrix (Version 0.92). Available from https://github.com/taiyun/corrplot.

Werner, I., 1997. Grazing of Arctic under-ice amphipods on sea-ice algae. Mar. Ecol. Prog. Ser. 160, 93–99.

Werner, I., 2005. Seasonal dynamics, cryo-pelagic interactions, and metabolic rates of Arctic and Baltic pack-ice and under-ice fauna. Universität Kiel, Kiel, p. 73. Habilitation thesis.

Werner, I., Hirche, H.-J., 2001. Observations on *Calanus glacialis* eggs under the spring sea ice in the Barents Sea. Polar Biol. 24, 296–298. https://doi.org/10.1007/s003000000202.

Wickham, H., 2007. Reshaping Data with the reshape Package. J. Stat. Softw. 21 (12), 1–20.

Wickham, H., 2016. ggplot2: Elegant Graphics for Data Analysis. Springer-Verlag, New York.

Wickham, H., et al., 2019. Welcome to the tidyverse. J. Open Source Softw. 4 (43), 1686. https://doi.org/10.21105/joss.01686.

Wickham, H., Hester, J., Chang, W., Bryan, J., 2022. devtools: Tools to Make Developing R Packages Easier. R package version 2.4.5, https://CRAN.R-project.org/package=devtools.

Wold, A., Assmy, P., Gradinger, R., Edvardsen, B., Goraguer, L., Wiktor, J., Tatarek, A., 2022. Ice algae biodiversity Nansen Legacy Q2 [Data set]. Norwegian Polar Institute. doi: 10.21334/npolar.2022.761bde20.